N O T I C E

THIS DOCUMENT HAS BEEN REPRODUCED FROM MICROFICHE. ALTHOUGH IT IS RECOGNIZED THAT CERTAIN PORTIONS ARE ILLEGIBLE, IT IS BEING RELEASED IN THE INTEREST OF MAKING AVAILABLE AS MUCH INFORMATION AS POSSIBLE

NASA Technical Memorandum 81505

COMPARISON OF SEVERAL INFLOW CONTROL DEVICES FOR FLIGHT SIMULATION OF FAN TONE NOISE USING A JT15D-1 ENGINE

J. G. McArdle, W. L. Jones,
L. J. Heidelberg, and L. Homyak
Lewis Research Center
Cleveland, Ohio

COMPARISON OF SEVERAL INFLOW CONTROL DEVICES FOR FLIGHT SIMULATION

OF FAN TONE NOISE USING A JT15D-1 ENGINE

by J. G. McArdle, W. L. Jones, L. J. Heidelberg, and L. Homyak
National Aeronautics and Space Administration
Lewis Research Center
Cleveland, Ohio 44135

Abstract

As part of a program to enable accurate simulation of in-flight fan tone noise during ground static tests, four devices intended to reduce inflow disturbances and turbulence were tested with a JT15D-1 turbofan engine. These inflow control devices (ICD's) consisted of honeycomb/screen structures mounted over the engine inlet. The ICD's ranged from 1.6 to 4 fan diameters in size, and differed in shape and fabrication method. All the ICD's significantly reduced the BPF tone in the far-field directivity patterns, but the smallest ICD's apparently introduced propagating modes which could be recognized by additional lobes in the patterns. All the ICD's had negligible transmission loss at low fan speeds; at supersonic fan tip speed the smallest ICD's had some measurable loss, but the largest had no loss. The JT15D-1 engine was found to have a tone source which generated a strong propagating mode at fan speeds corresponding to "approach" power and higher. This mode, which was not affected by an ICD, is associated with six structural struts behind the fan, but the exact noise producing mechanism was not identified. Two of the ICD's were tested with miniature dynamic pressure transducers mounted on the fan blades. Data from a typical transducer showed that the unsteady inflow distortion modes (turbulence) were eliminated or significantly reduced when either of the ICD's was installed. However, some steady inflow distortion modes remained; those that could result in propagating acoustic modes are believed to be related to lobes observed in the directivity patterns.

Introduction

Modern turbofan engines produce less noise in flight than in ground static tests. A major reason for this difference is fan tone noise which is generated by turbulence and other inlet flow distortions that are present in static testing but not in flight. Several investigators (refs. 1 to 7) have shown that honeycomb/screen structures mounted over the test inlet can reduce inflow disturbances and tone noise arising from the disturbances. In this report, a honeycomb/screen structure is called an "inflow control device" (ICD).

A research program is under way at NASA Lewis Research Center (LeRC) to better understand generation of fan tone noise, and to develop ICD's

E-443

and techniques to enable more accurate simulation of in-flight tone noise. The program is part of a NASA inter-center "Forward Velocity Effects on Fan Noise" program that involves static, wind-tunnel, and flight tests using the Pratt and Whitney of Canada JT15D-1 turbofan engine.

The principle objectives of the test program at LeRC are (1) to develop an ICD which minimizes tone noise components which are not present in flight; (2) to ensure that the ICD does not attenuate or redirect sound radiated from the engine to the far field; and (3) to provide as much design information as possible for similar devices for other engines. Further, the tests are aimed at developing an ICD which is small in size (less than 2 fan diameters), lightweight, simple, and inexpensive to build.

Some of the previous work at LeRC, including a method of judging the acoustic transmission characteristics of ICD's, is described in reference 1. Since that report, much additional progress has been made, but all the program objectives have not been fulfilled and more study remains to be done. This report describes and compares significant results of tests of four ICD's with different shapes, sizes, and fabrication techniques. Some results from tests using dynamic pressure transducers mounted on the fan blades are also included. The blade mounted transducers are a relatively new tool for acoustic investigations, and have been useful in evaluating the ICD performance, and in identifying some important tone sources.

Apparatus and Procedure

Engine and Facility

The JT15D-1 engine, sketched in figure 1, is a two-spool turbofan engine with nominal 3.3 bypass ratio. Important performance characteristics are given in table I. The fan is 53.3 centimeters (21.0 in.) diameter, and has 28 blades and 66 exit guide vanes in the bypass duct. (The 66 vanes are herein called the "fan stator"). The centrifugal core compressor has 16 blades. The engine used for these tests was an early production model. All parts were standard except the fan exit guide vanes in the core flow passage (herein called the "core stator"). The standard assembly (33 vanes) was replaced so that fan rotor/core stator interaction tones would be acoustically cut off. The new design has 71 thinner vanes, which also were set a little farther aft than the standard vanes. The vanes in the new core stator are 0.63 fan blade root chords aft of the trailing edge of the fan blade root, compared with 0.28 chords for the standard vanes.

On the JT15D-1, the core engine is supported from the outer case by a main frame consisting of six structural struts. The struts are located just aft of the stators, as indicated in figure 1.

For these tests several things were done to minimize unwanted noise which might be generated from facility or test configuration causes:

(a) Engine centerline height was 2.9 meters (9.5 ft), or 5.4 fan diameters above the ground. This height, measured in fan diameters, is larger than many engine test installations. It was chosen to attempt to minimize ground plane effects on the inlet flow.

(b) The engine was covered by a smooth cowling to minimize distortions in the air flowing from the rear into the engine inlet. The cowling was 107 centimeters (42 in.) in diameter, and had a circular cross-section. It was not intended to simulate an airplane nacelle. The forward part of the cowling could be changed to mount the different ICD's.

(c) The engine was suspended from the facility thrust system by a forward-facing cantilever arm which faired smoothly into the cowling. The engine was positioned on this arm so that the front of the inlet was not closer than 3.4 fan diameters to any facility structure.

(d) The inlet air temperature sensor (a rod-like part on the inlet wall) was retracted so that its wake did not make tone noise.

(e) The engine exhaust was connected to a large muffler to suppress aft fan noise and jet noise.

The tests were performed at the LeRC Vertical Lift Facility. The facility is an outdoor test stand sheltered by a service building which was moved away on tracks before testing. The area beneath the engine out to the far-field microphones was paved with concrete. A photograph of the test setup is shown in figure 2.

ICD and Inlet Configurations

The ICD's and inlets are sketched in figure 3, and shown in the photographs of figures 2 and 4 through 6. Some of the characteristics of ICD numbers 1 and 2 were reported in reference 1.

ICD number 1 (figs. 2 and 3(a)) was made of twelve 5-centimeter (2-in.) thick flexible ("Flex-Core") honeycomb panels laid over a coarse base screen and a fine-mesh turbulence reducing screen. The honeycomb cell length, ℓ, to equivalent diameter, d, ratio was approximately 8. Structural support and shaping was provided by equally spaced steel ribs 3 millimeters (0.125 in.) thick. For some tests' an additional fine-mesh screen of 12 joined sections, each similar in shape to the honeycomb panels, was installed inside the ICD. This screen was based on results of tests reported in reference 6. The additional screen was held tautly in place by several 10-centimeter (4-in.) long wires from each of the ribs, and thus approximated the shape of the inside surface of the ICD. This ICD was mounted over the cowling. The inlet lip was nearly semi-

4

circular in cross-section, and formed a bellmouth for the cylindrical inlet duct. Because of its weight, this ICD was supported by thin rods from an overhead facility structure. It was the only ICD tested which needed external support.

ICD number 2 (fig. 3(b)) was made of a single flat sheet of 10-centimeter (4-in.) thick honeycomb (cell $l/d \sim 11$). No supporting ribs were used. The ICD was mounted in the inlet duct just behind the bellmouth lip. Further description is given in reference 1. Also, in that reference this ICD was reported to cause acoustic transmission losses and changes in far-field directivity; consequently, the acoustic data are not discussed further in this report.

ICD number 3 (figs. 3(c) and 4) was made of four 5-centimeter (2-in.) thick fiberglass honeycomb sections (cell $l/d \sim 5$). The orange-peel shaped sections were heat formed over a mold, trimmed to size, then epoxied together (without ribs) at the mating edges of the sections. Thus, the mating edges were composed of randomly-cut cells, but the epoxied joints were reasonably uniform and were made neatly (see fig. 4(b)). The ICD cross-section contour was designed so the honeycomb cells were aligned with flow streamlines calculated by a potential flow analysis. The resulting shape was nearly hemispherical, and was self-supporting. The inlet lip used with this ICD was flat at the highlight, and faired into both the cowling and cylindrical inlet duct with circular arcs. The installed ICD fit into the flat area of the lip.

ICD number 4 (figs. 3(c) and 5) was made of eight 2.5-centimeter (1-in.) thick flexible honeycomb sections (cell $l/d \sim 4$). The orange-peel shaped sections were formed and trimmed over a mold, then the edges were epoxied to thin steel ribs which extended beyond the honeycomb faces. Adjacent ribs were spot welded together, forming a self-supporting structure. The inside contour of the honeycomb and the inlet were the same as for ICD number 3.

ICD number 5 (figs. 3(d) and 6) was made of six sections of 5-centimeter (2-in.) thick flexible honeycomb (cell $l/d \sim 8$). It was fabricated with thin ribs between the sections, similar to ICD number 4. In addition, a grid of 1.6 millimeter (0.063 in.) wires on approximately 5-centimeter (2-in.) centers was used for more support beneath the honeycomb (see fig. 6(b)). The inlet duct for this ICD was a conical diffuser duct rather than a cylinder as used with the other ICD's. The lip (taken from ref. 8) was elliptical in cross-section up to the highlight, then faired into a conical skin, which in turn faired into the cowling. The ICD was mounted on a machined ring in the conical section. The ICD contour was designed so the honeycomb cells were aligned with flow streamlines calculated by a potential flow analysis. A similar analysis showed that this inlet would be suitable for low-speed flight.

For the acoustic transmission tests, a 10-centimeter (4.0-in.) long spool piece was inserted between the front engine flange and the inlet

duct. Forty-one equally spaced, radially directed rods were mounted in this spool (see fig. 3(e)). Each rod was 0.5 centimeters (0.19 in.) diameter and 6.4 centimeters (2.5 in.) in length. The rods and spool piece were the same as reported in references 1 and 9.

Acoustic Instrumentation and Data Processing

Far-field noise measurements were made with 1.3 centimeter (0.5 in.) microphones located on the ground 27 meters (90 ft) from the engine. The microphones were spaced at 10-degree intervals from 10 to 120 degrees from the engine inlet axis.

The microphone data were recorded on magnetic tape and then processed on a spectrum analyzer. The results were corrected to 30.5-meter (100-ft) free-field radial distance, and standard-day temperature and relative humidity (15° C (59° F) and 70 percent, respectively). The correction applied to the ground microphone data to obtain free-field levels was -6.0 dB at all frequencies up to 20 kilohertz.

Blade Mounted Transducers

For some of the tests, dynamic pressure data were obtained with eight miniature transducers mounted on two of the fan rotor blades. A photograph of the instrumented blades is given in figure 7(a), and the transducer locations on the blades are shown in figure 7(b). Six transducers were mounted approximately 4 millimeters (0.16 in.) from the leading edge, and two were mounted approximately 9 millimeters (0.35 in.) from the trailing edge. All measured dynamic pressures on the "pressure" surface of the blade, except transducer B-4. For some of the tests (not reported herein) transducers were mounted on fan stator and core stator vanes.

The transducers were mounted as illustrated in figure 8. The mounting technique enables the transducers to operate properly under large radial acceleration loads. (For the JT15D-1, the maximum load is about 76 000 g at the fan blade tip). Fabrication details and response characteristics of the installed transducers are given in reference 10.

The pressure data were telemetered from transmitters in the nosecone to an antenna mounted in the inlet duct wall. The general arrangement of the system is shown in figure 9. Each transducer was coupled to its own FM transmitter. Transmitter circuitry gains were manufactured so that the output from each transducer was 1 volt rms for a 171-dB tone (re 2×10^{-5} Pa) applied to the pressure-sensitive diaphragm by a close-coupled acoustic driver. The whole system was powered by 10 lithium primary batteries.

6

The analog pressure signals were recorded, along with other test data, on magnetic tape. The recorded data were analyzed on a fast-Fourier-transform spectrum analyzer, and also digitized for further calculations with a specially written program for a digital computer.

In order to conserve the batteries, a special switch was used to energize system power only when data were being taken. The switch was activated by a strobe light located in the inlet duct wall. An optical sensor was used to indicate the passage of a designated fan blade during each fan rotor revolution. The indication is accurate to about 1 degree of rotation; it was used as a "trigger" signal for many of the blade mounted transducer data analyses. It was not feasible to calibrate the system before each test run. Thus, no calibration data were taken after installation until after the tests reported herein were completed. By then, the system had accumulated 4.6 engine run hours and 2.6 powered hours (including pre-test checkouts). At that time two transducer channels were not operating satisfactorily, and only two of the remaining six could be reached with the calibration signal source with the rotor on the engine. For those two channels, the output was within 1 dB of the expected calibration value.

Procedure

For all tests, data were obtained at three corrected fan speeds: 6750 (near idle power), 10 500 (near approach power), and 13 500 rpm (high power, supersonic fan tip speed). In most cases (including acoustic transmission tests with 41 rods in the inlet) tests were performed with, then without, an ICD on the same day to improve data quality. From the large quantity of data taken, representative results have been chosen to be presented at this time.

For all tests ambient wind was less than 8.7 knots (10 mph); for the tests with blade mounted transducers reported herein the ambient wind was nearly zero.

Results and Discussion

Effect of ICD on Engine Operation

When testing engines on outdoor stands, the fan speed usually wanders more or less slowly around the desired setting even though the fuel-flow rate and core speed are steady. The speed fluctuations have been observed to be associated with the wind. The same types of fluctuations have occurred with engines having different exhaust nozzle systems and bellmouths, and both with and without the muffler connected. It is believed that the fluctuations are caused by flow effects in the inlet duct, although no correlations with wind velocity have been made. However, with an ICD installed, the fan speed was always much steadier, as

shown in figure 10. Although the example given is ICD number 1, the results were the same for all ICD's tested.

The total-pressure loss for the ICD's tested is shown in figure 11. The inside surface flow area, A_{flow}, and the approximate through-flow velocity at 10 500 rpm fan speed, $V_{10\ 500}$, are also shown. The pressure loss, which is a function of the flow velocity squared, is highest for ICD number 2 (the flat, in-duct ICD), and quite low for the other ICD's. For tests with ICD number 2, the fan exhaust nozzle area was enlarged slightly to compensate for the inlet pressure loss. For the other ICD's, the pressure drop was so small that the engine operating line was not changed significantly, and no compensation was made.

Far-Field Acoustic Directivity Patterns

The discussion in this section and in following sections will use concepts and terminology from reference 9 and generally will consider only fan tones (i.e., no core compressor tones).

A specific acoustic mode is identified by its circumferential order, m, and radial order, μ, and commonly designated the (m,μ) mode. At subsonic tip speeds, modes are generated in the engine by interaction between rotating fan blades and various types of flow disturbances (e.g., turbulence or wakes in the incoming flow), or by rotor wakes interacting with vanes in the exit passage. Many modes are generated by the fan, but at each speed only some of them propagate out of the inlet into the far field. The modes that propagate are termed "cut-on", while those that do not are "cut-off". Modes of higher m and μ order become cut-on as the fan speed is increased. At the fan blade passing frequency (BPF) or one of the BPF harmonics, each propagating mode radiates acoustic energy in its own distinctive directivity pattern. Each pattern is lobular in shape, having one or more peaks. For modes near cut-off, the strongest peak (called the principal lobe) tends to be directed toward sideline angles. The principal lobe moves toward the inlet axis as the mode becomes fully cut-on. In the far field, the total acoustic energy at any given location is the summation of energies arriving from all the cut-on modes from all the sources. For the summation, the relative phasing of the modes determines whether the energies are numerically additive (in-phase) or subtractive (out-of-phase).

Data. - The far-field acoustic behavior was studied mainly with narrowband (25-Hz bandwidth) spectra, because one-third octave results often did not characterize tone behavior effectively. Typical spectra are shown in figure 12. The broadband noise level associated with the fan BPF is referred to frequently in the following discussion; this level was determined from the narrowband spectra by drawing the broadband line through the base of the BPF tone. Data are presented in figure 12 for tests with and without an ICD. With the ICD installed the fan BPF was

reduced, but the broadband level was the same. The core BPF was the same, as expected, because this tone is caused by wakes from the core engine support struts just ahead of the centrifugal compressor. Harmonic and other tones sometimes were changed, but no trends were established from this test program.

Far-field directivity patterns for ICD numbers 1, 3, 4, and 5 are shown in figures 13 through 15 for 6750, 10 500, and 13 500 rpm fan speeds, respectively. In each of the figures data are shown for tests with the ICD installed, and for the same inlet without the ICD. For these plots, the fan BPF tone and broadband level were determined from the narrowband spectra from each microphone, as described in the preceding paragraph, and have been corrected to free-field, 30.5-meter (100-ft) radius, standard-day conditions as described in the section "Acoustic Instrumentation and Data Processing". In general, the BPF tone was reduced with an ICD installed, but the broadband level remained the same. Tone level reduction over a wide angular range is attributed to significant reduction of interaction between the fan rotor and incoming turbulence or other inflow disturbances. This is the effect the ICD was intended to accomplish. However, additional tone peaks often appeared near the axis and at other angles for ICD numbers 3, 4, and 5, indicating that the presence of these ICD's caused new distortions which resulted in propagating modes strong enough to influence the directivity patterns. For ICD number 3 (and, probably, also ICD number 4 because it is nearly the same in size, shape, and mounting method) the new distortions are believed to be associated with honeycomb sections and joints in the ICD structure; these will be discussed in more detail with the blade mounted transducer data. No blade mounted transducer data are available for ICD number 5, and the reasons for the far-field results for this ICD are not yet clear. In addition to possible distortions from structural joints, it is also possible that distortions were produced in the flow along the cowling near the base of the ICD, or in the flow around the sharper lip (see fig. 3(d)), as suggested in reference 11.

At 6750 rpm fan speed, all modes having circumferential order higher than m = 14 are cut-off. As shown in figure 13, the BPF tone was almost reduced to the broadband level for ICD number 1, showing that this ICD effectively removed the incoming flow disturbances and did not produce significant new modes at this speed. The other ICD's also reduced the tone at most angles. For ICD numbers 3 and 4, a strong new lobe can be seen near the axis, and a weaker lobe around 110°. As discussed in the preceding paragraph, these lobes are presumed to represent modes caused by these ICD's, because they did not appear with ICD number 1.

At 10 500 rpm fan speed, all modes having circumferential order higher than m = 23 are cut-off. As shown in figure 14, the tone was reduced throughout the far field for all ICD's (except at angles near the axis for ICD numbers 3 and 4). This general overall reduction again indicates that the ICD's removed the inflow distortions. For example, when ICD number 1 was installed, the tone was reduced to broadband level

(or lower) near the axis, and at other far-field angles the tone was sufficiently reduced to expose a strong lobe peaking near 60° (except for ICD number 4, for which no good explanation is known). This lobe is atrributed to an engine generated mode of circumferential order $m = 22$, which becomes cut-on at about 9600 rpm fan speed. This mode is associated with interaction between the 28 fan blades and the six downstream structural struts, and will be discussed in more detail in other sections of this paper. Results for ICD number 5 are similar to those for ICD number 1 except for an indication of a possible new lobe peaking near 20°. For ICD numbers 3 and 4, the ICD-related tones noted at 6750 rpm fan speed now peak nearer the axis, as expected from theory because of the increased rotor speed.

At 13 500 rpm fan speed the rotor tip relative velocity is super-sonic, and strong rotor-locked modes are produced in the engine and pro-pagate toward sideline angles. As shown in figure 15, the tone level was reduced near the axis for ICD numbers 1 and 5, but not at angles greater than about 50° for ICD number 1. This characteristic is expected because there is no reason for the ICD to affect the tone when it is generated by a source not related to inflow distortions. With ICD numbers 3 and 4, the tone level was reduced at higher angles, suggesting some ICD transmission loss (discussed further in the next section). Also, some unexpected and unexplained peaks and valleys occurred. It is possible that propagating modes were produced by interaction with distortions related to flow near the base of the ICD at the inlet lip (see ref. 11). Also, it is possible that the method of attaching these ICD's to the bellmouth lip (see fig. 3(c)) caused a change in the effective acoustic length of the inlet. This, in turn, may have led to changes in strength and phasing of the energy radiated to the far-field lobes. This idea was introduced in reference 9, where it was discussed in relation to a test in which the inlet length was purposely changed. Again, in fig-ure 15, the broadband level both with and without ICD number 5 was the same but was shifted toward sideline angles by as much as 20° (compared to ICD number 1; see fig. 15(d)). The same shift can be seen in the tone directivity patterns, indicating that this inlet affected acoustic energy radiation to the far field in a different way than the bellmouth-like in-lets at higher fan speeds.

For a few tests an additional turbulence-reducing screen was in-stalled inside ICD number 1 (see fig. 3(a)). As shown figure 16, the performance of this configuration was essentially the same as ICD num-ber 1 without the additional screen.

Transmission Characteristics

For the acoustic transmission tests a set of 41 rods protruding radially from the inlet wall was placed in the engine just ahead of the fan. Wakes from these rods interacted with the fan blades to provide a strong new source consisting of $m = 13$ modes (see ref. 9). The BPF

tone from this source appeared as a dominant peaked lobe in the far-field directivity pattern. For most tests this lobe was so strong that it was not affected by the tone from rotor/inflow distortion interaction. By comparing the pattern with and without each ICD installed, the level near the peak of the dominant lobe indicated any transmission loss that might have occurred as the acoustic energy passed through the ICD. The testing technique is the same used for the tests reported in references 1 and 9. However, the present results were evaluated using narrowband rather than one-third-octave spectra as was done previously. For ICD number 1 only, the data given in this section of the report were obtained using the production core stator (33 vanes).

Results of the acoustic transmission tests are shown in figures 17 through 19 for 6750, 10 500, and 13 500 rpm fan speeds, respectively. The data for the same inlet configuration, but without the 41 rods or the ICD, are shown on each figure for comparison. In general, a dominant lobe from the rod wake/rotor interaction source is easily seen. However, the rods somehow affected other sources in the engine, because the tone level increased near the axis where there are no lobes from rod-related modes. For example, in figure 17(b) the tone without the ICD installed increased by approximately 5 dB with the rods. In addition, the broadband level unexpectedly increased when the rods were installed, especially at the highest speed. The reasons for these effects are not understood, but they do not change interpretation of the test results in the vicinity of a dominant peak.

Results of tests at 6750 rpm fan speed are shown in figure 17. At this speed a dominant lobe due to the (13, 0) mode peaked near 60°. Only small changes in the lobe were measured when each ICD was installed. These results are interpreted to mean that the ICD's caused little or no transmission loss at this speed.

Results of tests at 10 500 rpm fan speed are shown in figure 18. At this speed a dominant lobe peaked near 40°; this lobe is caused by the (13, 0) mode although modes of higher radial order are also cut-on. As with the tests at 6750 rpm the data near the dominant peak are judged to be reasonably alike both with and without each ICD installed; therefore, the ICD's caused little or no transmission loss at this speed.

Results of tests at 13 500 rpm fan speed are shown in figure 19. At this speed many modes are cut-on, including the (13, 0) through (13, 4) modes and the (28, 0) mode from the supersonic-tip-speed rotor. The principal lobe from the (13, 0) mode peaked near 25°, as can be seen for the test with ICD number 1 (fig. 19(a)). For the other tests, the area between that peak and the peak for the (28, 0) mode near 60° tended to "fill in" with energy from other propagating modes. Absence of a dominant lobe makes quantitative interpretation of the results difficult. However, the tone levels near 25° seem to be generally lowered when either ICD number 3 or 4 is installed, so these ICD's are considered to exhibit some transmission loss. This judgment is consistent with results

of the directivity tests discussed with figures 15(b) and (c) in the preceding section. With ICD number 5, the peak may have been redirected slightly toward the sideline, but transmission losses cannot be determined from these data.

Evidence for m = 22 Mode

The directivity pattern for the engine with ICD number 1 is shown again in figure 20 for 10 500 rpm fan speed. The theoretical directivity pattern for the (22, 0) mode is also shown by a dashed line. This is the only mode of circumferential order 22 which can propagate in the inlet duct at this fan speed. The m = 22 mode could come from rotor wake (28 blades) interaction with the six structural struts. The principal lobes for the experimental and theoretical patterns peak at nearly the same far-field angle, and have very similar shapes. Sketches of amplitude probability density function (PDF) plots obtained for the 20° and 60° far-field microphones are also shown in the figure. At 20° the PDF plot indicates tone amplitude variations from a mainly random source, but at 60° the plot indicates a tone source having much periodic content. The periodic ("steady") tone suggests a steady interaction source in the engine, while the random source suggests residual inflow turbulence or reduction of the tone to nearly broadband level. At 6750 rpm fan speed (not shown in fig. 20) the PDF plots showed random tone sources at all far-field angles, as expected because the m = 22 mode is cut-off at that speed.

Further evidence for this mode was obtained in a special test illustrated in figure 21. As shown by the sketch, two dynamic pressure transducers were mounted in the same plane in the inlet duct and spaced 1/44 of the duct circumference apart. This spacing is equivalent to one-half the circumferential wavelength of the m = 22 mode. The signals were filtered at the fan BPF and displayed together on an oscilloscope. One of the signals was used to trigger both displays. As can be seen from the photograph of the scope screen, the signals are 180° out-of-phase, as expected for a spinning mode having 22 equally-spaced pressure lobes.

Tests with Blade Mounted Transducers

Tests with blade mounted transducers have been performed with no ICD, with ICD number 1 (with and without the additional screen installed; see fig. 3(a)), and with ICD number 3. Unless stated otherwise, in this discussion the data from transducer B-3 (near the leading edge of the pressure surface, 2 centimeters (0.75 in.) from the tip; see fig. 7(b)) are presented for 10 500 rpm corrected fan speed. This transducer is outside the calculated thickness of the boundary layer on the inlet duct wall. These results appear to be representative of results from the

other transducers. The tests were performed when the ambient wind was nearly zero at the test site.

A blade mounted transducer senses changing pressure on the blade surface. The changing pressure may be an aerodynamic (flow related) pressure, or an acoustic pressure, or a mixture of both. If the changing pressure is aerodynamic, it is caused by a velocity perturbation in the incoming airflow. The perturbation is here called a distortion. A distortion may be random or spatially steady. The common example of a random distortion is inflow turbulence, which can occur at any place in the inlet; turbulence which produces significant tone noise must exist for several fan revolutions. Examples of spatially steady distortions are inlet strut wakes, or potential fields extending forward from downstream obstructions such as vanes. If the changing pressure sensed by the transducer is an acoustic pressure, it could result from being in the near field of sources on the blades generating tone noise by interaction with a distortion, or it could be a spinning acoustic mode generated by rotor wake interaction with downstream vanes or struts. The blade transducer senses the propagating acoustic modal pressure pattern the same as if it were caused by spatially steady distortions, because the modal pattern spins at a fixed speed relative to the rotor. Thus, from these data there is no way to distinguish between acoustic pressures and spatially steady distortions, and at the present time it has not been determined whether the blade mounted transducer data represent mainly aerodynamic or mainly acoustic pressure sources. It is important ultimately to define the sources so that the noise generating mechanisms can be identified. However, the nature of the pressure sources is not critical for purposes of this report because, as will be brought out in the following discussion, most of the conclusions are the same no matter which way the data are interpreted.

Signal-enhanced pressure. - Pressure variations caused by random distortions can be removed from the total transducer signal by conventional signal enhancement techniques, using the optical blade sensor described in the "Apparatus" section for the trigger. During enhancement, the pressure changes from unsteady disturbances tend to cancel out. The enhanced pressure waveform obtained from an ensemble average over 200 revolutions is shown in figure 22 for a test with ICD number 1. This trace represents the averaged pressure changes measured by the transducer as it rotates around the inlet. As illustrated, the enhanced pressure trace consists of three superimposed patterns: (1) a once-per-revolution variation which indicates a flow difference between the top and bottom of the duct; (2) a six-per-revolution variation, which is associated with the six structural struts behind the fan stator; and (3) a 66-per-revolution variation, which is associated with the 66 fan stator vanes. (For transducer B-8, near the hub, this variation is 71-per-revolution, which is associated with 71 core stator vanes.) Thus, the transducer measured a complex pressure field which may contain acoustic pressures as well as effects of real flow distortions, but which never-

theless contains much information regarding engine-generated tone noise sources.

Blade pressure spectrum without ICD. - The narrowband (6.25-Hz BW) spectrum of the blade mounted transducer signal for a test without an ICD is shown in figure 23. The spectrum consists of spikes at the shaft rotational frequency and its harmonics all standing on a broadband base. The base is 10 to 15 dB higher than the broadband level measured by a transducer on the duct wall. Assuming that the transducer senses aerodynamic pressures, the spectrum represents the Fourier decomposition of the circur rential variations in the flow field at the fan face. On this assumption, the second abscissa scale is given. This scale shows the circumferential inflow distortion mode number, q. As in reference 12, q represents all the inflow distortions and their harmonic components. The third abscissa scale is the circumferential acoustic mode number, m, for the BPF tone. This scale defines the circumferential order of a spinning acoustic mode caused by interaction of the qth distortion mode with 28 blades ($m = NB - q$, where N is 1 for the BPF tone and B is the number of fan blades). As mentioned previously, it cannot be determined if the spikes really represent inflow distortions, or, alternatively, if they are due to acoustic pressures. Either source could yield the observed spectrum, except that propagating acoustic modes cannot cause the spikes for q less than 5 (m greater than 23) because those modes are cut-off.

These data support the currently popular hypothesis that tone noise is produced when the fan blades chop through distortions in the incoming flow. Both spatially steady distortions and unsteady distortions may be present in the inlet; the unsteady distortions are usually elongated eddies originating from random atmospheric turbulence which is "stretched" as it accelerates through the inlet during ground tests. Any number of eddies and steady distortions may exist at various locations in the inlet at any given time. Each distortion affects the local flow velocity and has an irregular profile, so appears to the fan as a distortion plus many harmonics. Collectively, all the distortions and their harmonics are called distortion modes; they are shaft ordered because the fan blades cross each distortion once every revolution. The fan blades interact with the distortion modes to produce tone noise on the blades in the manner discussed in reference 12. The tone noise, in the form of acoustic modes, radiates in all directions from the blades. Cut-on modes propagate through the fan ducts and radiate acoustic energy to the far field.

Blade pressure spectrum with ICD number 1. - The blade pressure spectrum for a test with ICD number 1 installed is shown in figure 24. The most significant peaks standing above the broadband floor are at q = 1, 2, 6, 12, 66, and 71 (the last two are not shown in fig. 24). In order to determine if these peaks are from random or steady sources, a narrowband spectrum of the enhanced pressure trace (fig. 22) was made and is presented in figure 25. This trace shows only the steady variations because the random variations cancel out during the enhancing

process. Comparison of figures 24 and 25 shows that the peaks are the same. Therefore, it is concluded that the peaks which were reduced below the broadband level were related to random distortions. The only known sources of random distortion in this test are inflow disturbances, as discussed previously. It follows that this ICD effectively removed the random inflow disturbances and, thus, the tone noise generated by rotor/turbulence interaction at this fan speed. This result is the same no matter how much acoustic pressure is contained in the transducer signal, and complements the analysis of the far-field acoustic performance discussed with figure 14. However, some steady distortion modes are still present to produce tone noise, and these will now be examined in more detail.

The peaks at $q = 1$ and 2 changed slightly when the ICD was installed. They were expected to diminish slightly, on the assumption that the ICD removed some random distortion at all q numbers. The $q = 1$ peak is believed to be caused by a top-to-bottom flow difference in the inlet, and the $q = 2$ peak is probably its harmonic. The small changes for these peaks show that this ICD (low-pressure drop; see fig. 11) did little to improve the mean flow uniformity. These distortions lead to modes which become cut-on near sonic tip speed. There is no way to judge, from the data obtained in this test program, whether these modes are strong enough to influence the far-field noise when the tip speed is supersonic. It is interesting to note, however, that the apparent flow non-uniformity was present in this test setup, which was built with the engine centerline 5.4 fan diameters above the ground and with the inlet well forward of any test stand structure. The pressure level measured by the transducer was greater near the bottom of the inlet (see fig. 22). This means that the flow rate was less than the average rate near the bottom, probably an effect of the ground plane.

The $q = 6$ peak was unchanged when the ICD was installed. This peak may be caused by the transducer passing through the potential field from the six struts supporting the core engine, or may be from an $m = 22$ mode propagating forward from rotor wake interaction with those struts. The $q = 12$ peak may be a harmonic of the $q = 6$ peak; or, it may be a new $q = 12$ distortion pattern produced by ICD number 1 (made in 12 sections). The $q = 66$ peak (not shown in fig. 25) may be caused by the transducer passing through the potential fields from the 66 fan stator vanes, or may be an $m = -10$ mode coming from rotor wake interaction with the vanes. The $m = -10$ mode is at the second harmonic of the fan BPF, and is the first rotor/stator mode cut-on at this fan speed. The $q = 71$ peak (not shown in fig. 25), which measures 20 dB less than the $q = 1$ peak, seems to be related to the 71 core stator vanes. It is difficult to consider that this peak is caused by real distortions because the core stator is located about 10 centimeters radially inward from this transducer. This peak probably consists mainly of acoustic pressures.

15

Blade pressure spectrum with ICD number 3. - The blade pressure
spectrum for a test with ICD number 3 installed is shown in figure 26.
In this plot, pressure peaks stand out at the same q numbers as for
ICD number 1 (see fig. 24), and observations previously made regarding
those peaks are applicable here also. The strengths of these peaks, as
well as the broadband floor level, are the same as for ICD number 1.
However, new peaks also appeared. Many of the new peaks had strong
steady components, as can be seen in figure 27, which is a narrowband
spectrum of the enhanced pressure trace. The strongest new peaks are at
q = 12, 16, 20, and 24. These peaks lead to modes which propagate in
directions near the axis at this fan speed and which probably account
for the far-field directivity shown in figure 14(b). The source of
these peaks has not been determined, but the fact that they are mul-
tiples of 4 suggests that the source is somehow related to the four
sections of honeycomb used to fabricate this ICD (see fig. 3(c)), even
though there is not a strong peak at q = 4. For many of the other
peaks, the strength from random sources tended to be greater with ICD
number 3 than with ICD number 1, if the strengths from random and steady
sources are additive. For example, at q = 15 the strength of the
random source is 127 dB - 120 dB = 126 dB for ICD number 3, and
124 dB - 118 dB = 123 dB for ICD number 1. This trend persists for q
numbers higher than 4, indicating that the residual random inflow dis-
turbances were greater with ICD number 3 than with ICD number 1. It
could not be determined how much these residual disturbances influenced
the far-field tone levels relative to the steady distortion modes intro-
duced with this ICD.

Concluding Remarks

Acoustic tests of four inflow control devices (ICD's) were made
with a JT15D-1 turbofan engine. The ICD's were honeycomb/screen struc-
tures mounted over the engine inlet. They ranged from 1.6 to 4 fan di-
ameters in size, and differed in shape and fabrication method. The test
results were evaluated by comparing the far-field BPF tone directivity
patterns with and without each ICD installed. In addition, rods were
mounted in the engine inlet for some tests to generate strong propagating
modes to judge whether the ICD's affected noise transmission to the far-
field.

All the ICD's significantly reduced the BPF tone caused by interac-
tion between the fan rotor and inflow disturbances and turbulence. The
largest ICD reduced the tone from this source throughout the far field,
and did not affect noise transmission. The smallest ICD's apparently
introduced propagating modes, which could be recognized by additional
lobes in the directivity patterns. Some of these modes are believed to
be due to inflow disturbances from joints or panels used in the ICD con-
struction. The smallest ICD's had no significant transmission loss at
lower fan speeds, but exhibited some loss at supersonic fan tip speed.
These faults may make the smallest ICD's (as built and attached to the

engine for these tests) unsuitable for fan acoustic testing. An ICD of intermediate size showed promising characteristics, but additional data are needed to complete evaluation of its performance.

The JT15D-1 engine appears to have a strong tone source which generates a propagating mode at fan speeds higher than 9600 rpm. In the far-field directivity pattern, the mode is clearly seen by a prominent lobe near 60°. The exact source was not identified but is believed to be either interaction between the fan blades and potential fields from six structural struts behind the fan, or rotor wake interaction with those struts.

Tests with miniature dynamic pressure transducers mounted on the fan blades were made without an ICD, and with the largest and smallest ICD's. Data from a typical blade mounted pressure transducer corroborated and clarified results of the far-field tests. In particular, narrowband spectra of the pressure signal showed that the ICD's removed unsteady inflow disturbances (turbulence) and their harmonics, and tended to leave only steady distortions related to the test setup, the six engine struts, and the IOD. Distortions from the test setup (probably the ground plane) caused modes which propagate only at high fan tip speed. Distortions from the smallest ICD caused modes which probably account for the additional lobes measured in the directivity pattern when it was installed. The blade mounted transducer data may contain acoustic as well as aerodynamic pressure components, but the presence of acoustic components should not affect the conclusions drawn from these data.

References

1. Jones, W. L., McArdle, J. G., and Homyak, L., "Evaluation of Two Inflow Control Devices for Flight Simulation of Fan Noise Using a JT15D Engine," AIAA Paper 79-0654, Mar. 1979.

2. Shaw, L. M., Woodward, R. P., Glaser, F. W., and Dastoli, B. J., "Inlet Turbulence and Fan Noise Measured in an Anechoic Wind Tunnel and Statically with an Inlet Flow Control Device," NASA TM-73723, 1977.

3. Woodward, R. P., Wazyniak, J. A., Shaw, L. M., and MacKinnon, M. J., "Effectiveness of an Inlet Flow Turbulence Control Device to Simulate Flight Fan Noise in an Anechoic Chamber," NASA TM-73855, 1977.

4. Hodder, B. K., "An Investigation of Possible Causes for the Reduction of Fan Noise in Flight," AIAA Paper 76-585, July 1976.

5. Ho, P. Y., Smith, E. B., and Kantola, R. A., "An Inflow Turbulence Reduction Structure for Scale Model Fan Testing," AIAA Paper 79-0655, Mar. 1979.

6. Kantola, R. A., and Warren, R. E., "Reduction of Rotor-Turbulence Interaction Noise in Static Fan Noise Testing," AIAA Paper 79-0656, Mar. 1979.

7. Ginder, R. B., Kenison, R. C., and Smith, A. D., "Considerations for the Design of Inlet Flow Conditioners for Static Noise Testing," AIAA Paper 79-0657, Mar. 1979.

8. Abbott, J. M., Diedrich, J. H., and Williams, R. C., "Low-Speed Aerodynamic Performance of 50.8-cm Diameter Noise-Suppressing Inlets for the Quiet, Clean, Short-Haul Experimental Engine (QCSEE)," (Proj. FEDD.) NASA TP-1178, 1978.

9. Heidmann, M. F., Saule, A. V., and McArdle, J. G., "Analysis of Radiation Patterns of Interaction Tones Generated by Inlet Rods in the JT15D Engine," NASA TM-79074, 1979.

10. Englund, D. R., Grant, H. P., and Lanati, G. A., "Measuring Unsteady Pressure on Rotating Compressor Blades," NASA TM-79159, 1979.

11. Woodward, R. P. and Glaser, F. W., "Effect of Inflow Control on Inlet Noise of a Cut-On Fan," AIAA Paper 80-1049, June 1980.

12. Kobayashi, H. and Groeneweg, J. F., "Effects of Inflow Distortion Profiles on Fan Tone Noise Calculated Using a 3-D Theory," AIAA Paper 79-0577, Mar. 1979.

TABLE I. - JT15D-1 ENGINE CHARACTERISTICS

Corrected to sea-level-static conditions

	Fan speed, rpm			Takeoff rating
	6750	10 500	13 500	
Thrust, N (lb)	1450 (325)	3690 (830)	6940 (1560)	9790 (2200)
Inlet airflow, kg/sec (lb/sec)	13.6 (30.0)	21.5 (47.5)	28.7 (63.3)	34.0 (75.0)
Fan pressure ratio	1.074	1.191	1.358	1.512
Fan tip Mach number	0.556	0.868	1.127	1.300
Fan tip relative Mach number	0.583	0.917	1.200	1.396
Cut-off ratio for BPF, rotor/fan vanes	0.40	0.63	0.86	1.06
Bypass ratio	3.37	3.31	3.18	3.05
Core speed, rpm	19 300	25 100	28 200	30 600
Fan BPF, Hz	3150	4900	6300	7210
Core BPF, Hz	5150	6690	7520	8160

FACILITY
SUPPORT

107-cm (42-in.)
DIAM COWLING

BEAM

6 STRUCTURAL
STRUTS

SECTION A-A

28 FAN BLADES

16 CORE COMPRESSOR BLADES

71 CORE STATOR VANES

66 FAN STATOR VANES
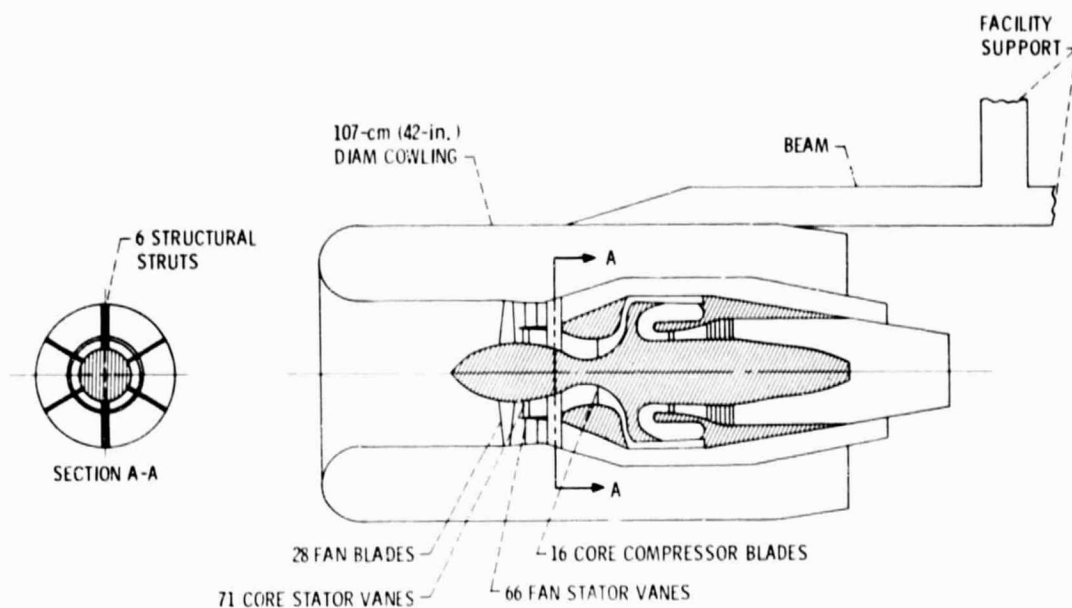
Figure 1. - Cross-section sketch of JT15D-1 test configuration.

C-78-1060
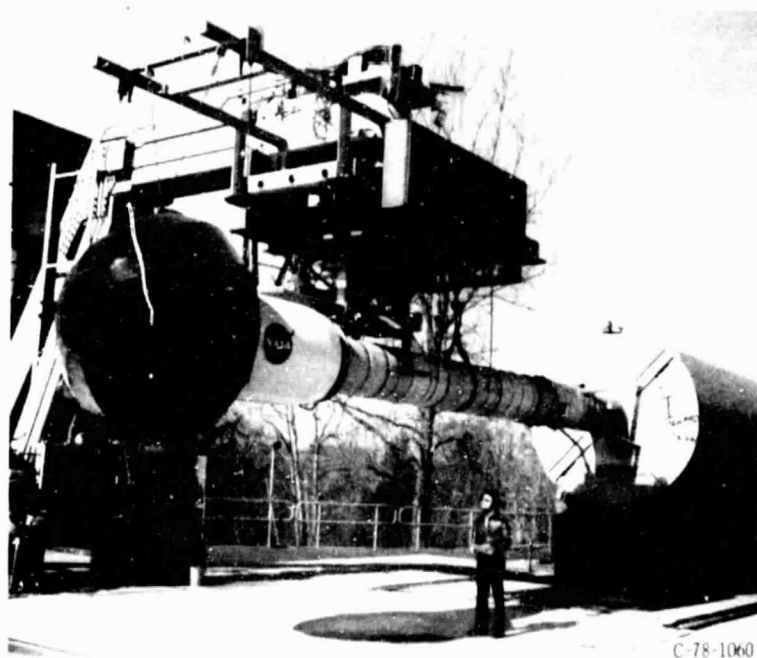
Figure 2. - JT15D-1 engine with ICD no. 1 installed on test stand with exhaust muffler.

5 cm (2 in.) "FLEXCORE" HONEYCOMB, 0.6 cm (1/4 in.) EQUIVALENT CELL SIZE

0.64 cm GRID BASE SCREEN AND 0.13 cm GRID TURBULENCE REDUCING SCREEN

ADDITIONAL TURBULENCE - REDUCING SCREEN (WHEN USED)

10 cm (4 in.)

ADDITIONAL SCREEN (WHEN USED)
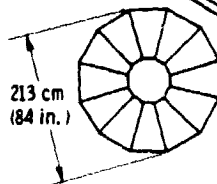
213 cm (84 in.)

FRONTAL VIEW

(a) ICD NO. 1.

10 cm (4 in.) HONEYCOMB, 1 cm (3/8 in.) CELL SIZE
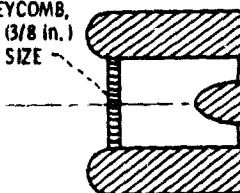
COWLINC

53.3 cm (21 in.)
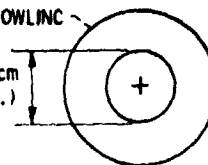
FRONTAL VIEW

(b) ICD NO. 2.

FOR ICD NO. 3: 5 cm (2 in.) FIBERGLASS HONEYCOMB, 1 cm (3/8 in.) CELL SIZE

FOR ICD NO. 4: 2.5 cm (1 in.) "FLEX CORE" HONEYCOMB, 0.6 cm (1/4 in.) EQUIVALENT CELL SIZE

90 cm (35.4 in.)

85 cm (33.4 in.)
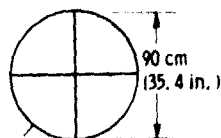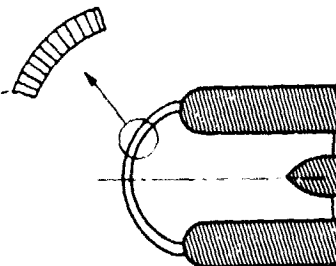
ICD NO. 3

ICD NO. 4

4 SECTIONS JOINED AT EDGES

8 SECTIONS JOINED WITH THIN RIBS AT EDGES

FRONTAL VIEWS

(c) ICD NOS. 3 AND 4.

Figure 3. - ICD and inlet configurations.

5 cm (2 in.)
"FLEXCORE"
HONEYCOMB,
0.6 cm (1/4 in.)
EQUIVALENT
CELL SIZE

SUPPORTING GRID,
1.6 mm (1/16 in.)
WIRE

105 cm
(41.3 in.)

6 SECTIONS JOINED
WITH THIN RIBS AT
EDGES

FRONTAL VIEW

(d) ICD NO. 5.

41 RODS, 0.5-cm
(3/16-in.) DIAM
6.4 cm (2.5 in.)
RADIAL IMMERSION,
EQUALLY SPACED
ON WALL

SPOOL
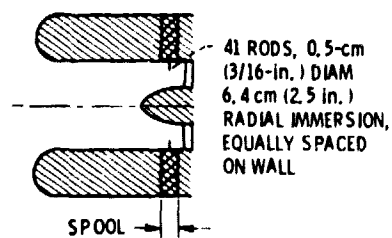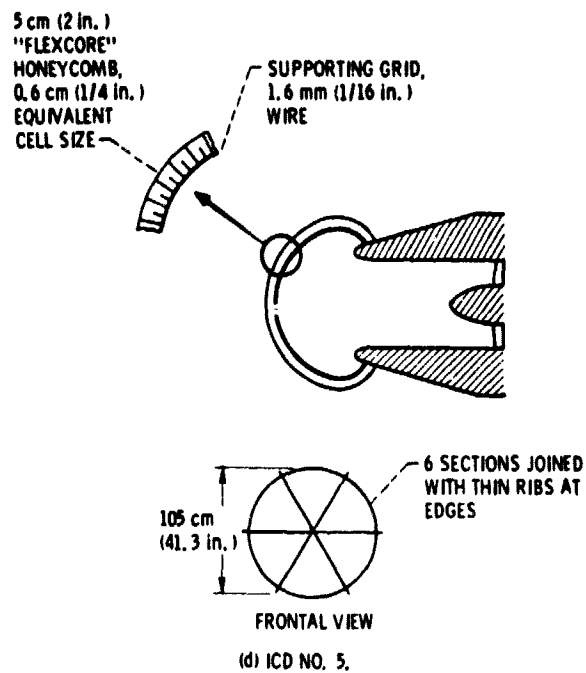
(e) 41-ROD ARRANGEMENT FOR ACOUSTIC
TRANSMISSION TESTS.

Figure 3. - Concluded.

C-78-4403
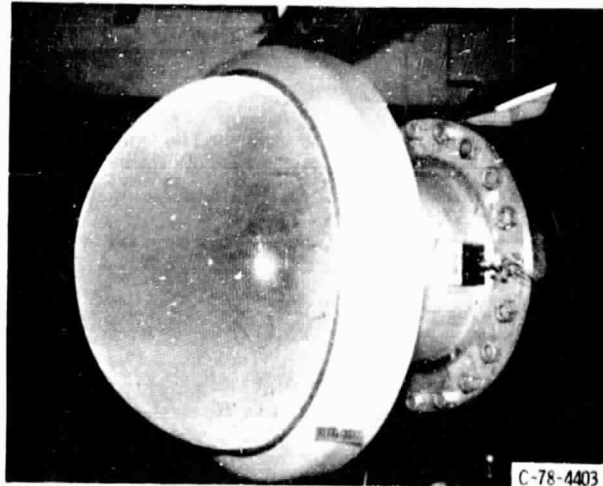
(a) ICD INSTALLED ON FLOW TEST RIG.

C-80-0675
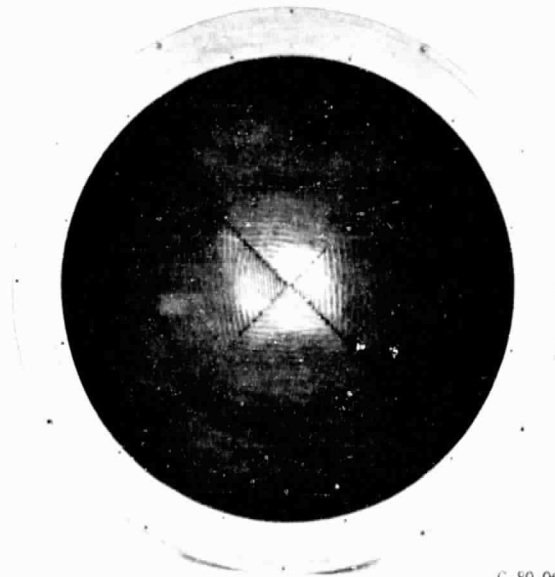
(b) VIEW LOOKING UPSTREAM, SHOWING JOINTS BETWEEN HONEYCOMB
SECTIONS.
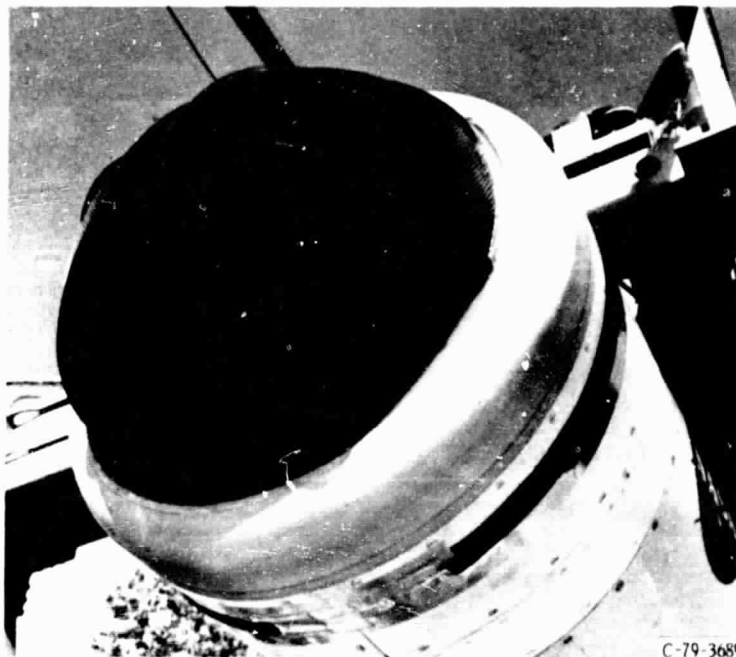
Figure 4. - ICD no. 5.

Figure 5. - ICD no. 4, showing thin ribs joining honeycomb sections.

C-79-3685

(a) INSTALLED ON ENGINE, SHOWING RIBS JOINING HONEY-
COMB SECTIONS, AND CONICAL COWLING.

(b) VIEW LOOKING UPSTREAM, SHOWING WIRE GRID SUPPORTING
HONEYCOMB SECTIONS.

Figure 6. - ICD no. 5.

(a) INSTRUMENTED BLADES.
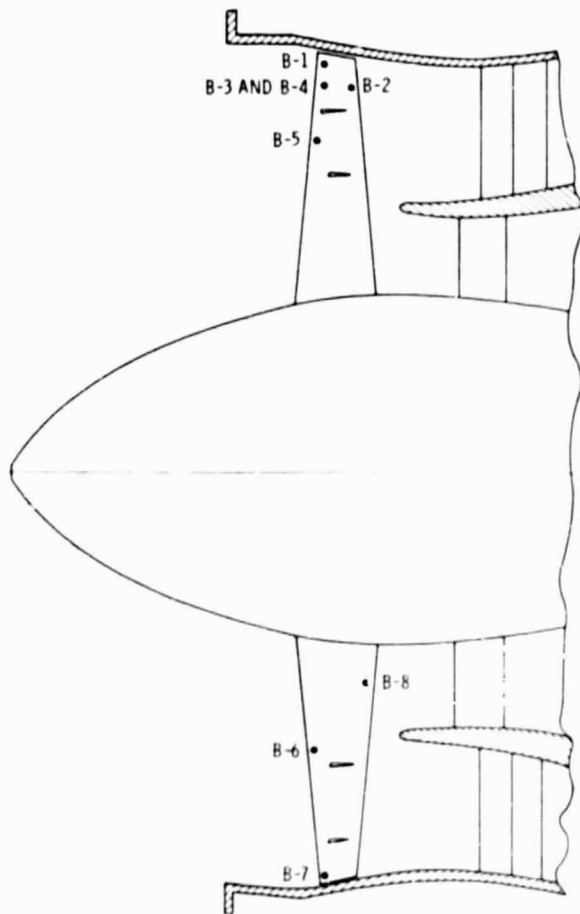
Figure 7. - Blade mounted pressure transducers.

TRANSDUCER	DISTANCE FROM WALL, cm (in.)	SURFACE MEASURED	MOUNTING STYLE
B-1	0.64 (0.25)	PRESSURE	SURFACE
B-2	1.90 (0.75)	↓	↓
B-3			
B-4	↓	SUCTION	
B-5	5.08 (2.00)	PRESSURE	
B-6	8.89 (3.50)		
B-7	0.64 (0.25)	↓	HOLE
B-8	12.7 (5.00)	↓	SURFACE

(b) TRANSDUCER LOCATIONS.

Figure 7. - Blade mounted pressure transducers.

RADIAL DIRECTION

1.55 mm

RTV

TRANSDUCER · 0.025 mm
HOUSING · THICK SHIM

PRESSURE SENSITIVE
DIAPHRAGM

EPOXY

BRASS SHIM

LEADWORK EXIT
THROUGH SHIM

0.5 mm

(b) HOLE MOUNT.

0.37 mm
MAX

RTV

EPOXY FILLET

RADIAL DIRECTION

TRANSDUCER HOUSING

PRESSURE-SENSITIVE DIAPHRAGM
WITH 0.025 mm RTV OVERCOAT

EPOXY

(a) SURFACE MOUNT.

Figure 8. - Methods of mounting pressure transducers on fan blades.
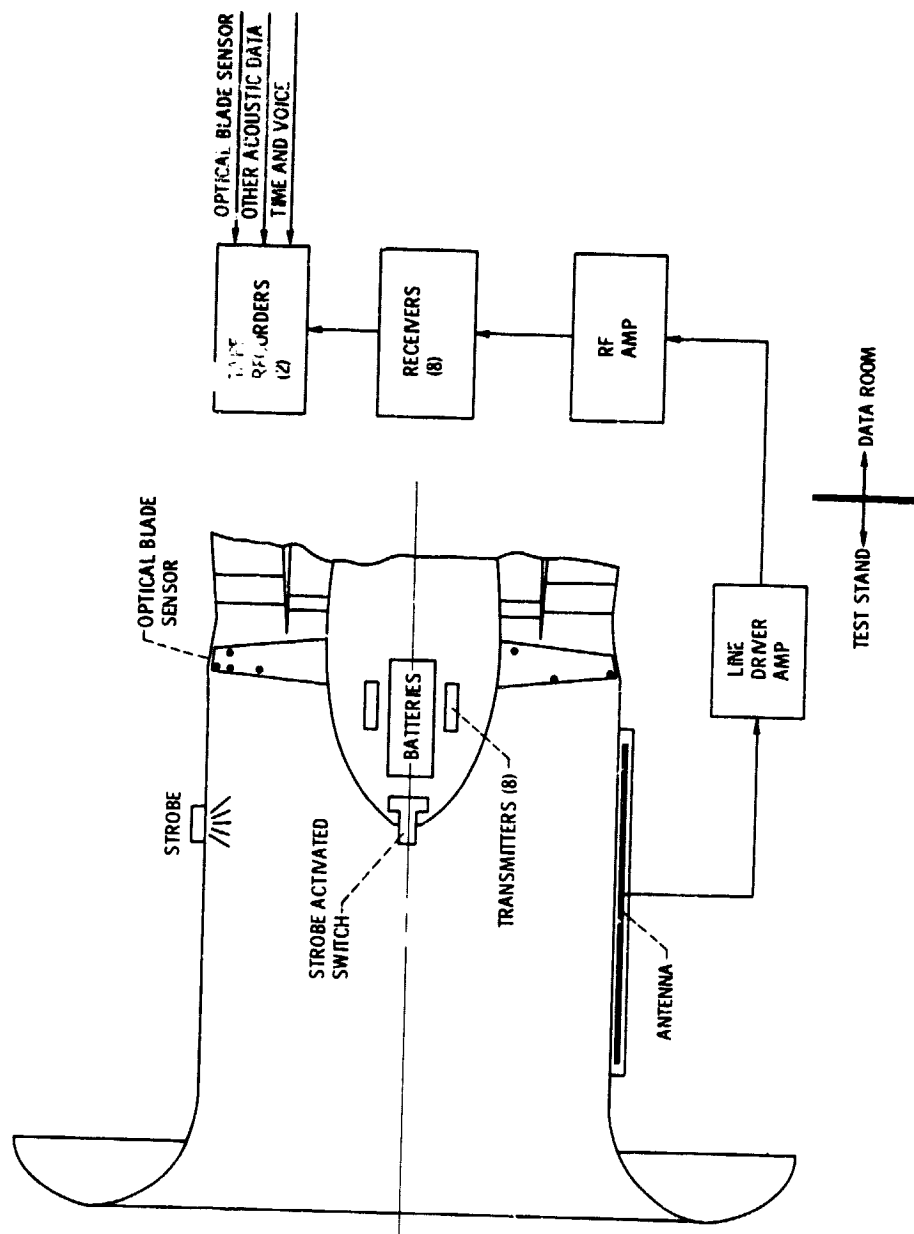
Figure 9. - Telemetry system for blade mounted pressure tranducer data.

CORE SPEED
FAN SPEED
300 rpm
|←1 min→|

(a) NO WIND.

NO ICD   WITH ICD

(b) 3.5 m/sec (8 mph) CROSSWIND.
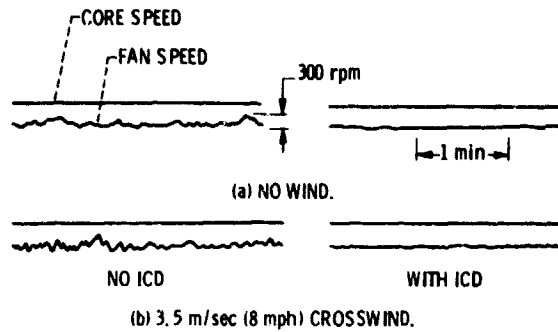
Figure 10. - Effect of ICD on fan speed steadiness. Fan speed approximately 15 000 rpm, ICD no. 1.

ICD NO.		A_{FLOW}		$V_{10\,500}$	
		m^2	ft^2	m/s	ft/s
○	1	9.2	99	2	6
□	3	0.8	8.7	22	71
◇	5	1.9	20	9.3	31
△	2 (REF. 1)	0.2	2.4	78	260

TOTAL PRESSURE LOSS, $\Delta P/P_{FREE\ STREAM}$, percent

INLET AIRFLOW CORRECTED TO STANDARD CONDITIONS, kg/sec

INLET AIRFLOW CORRECTED TO STANDARD CONDITIONS, lb/sec
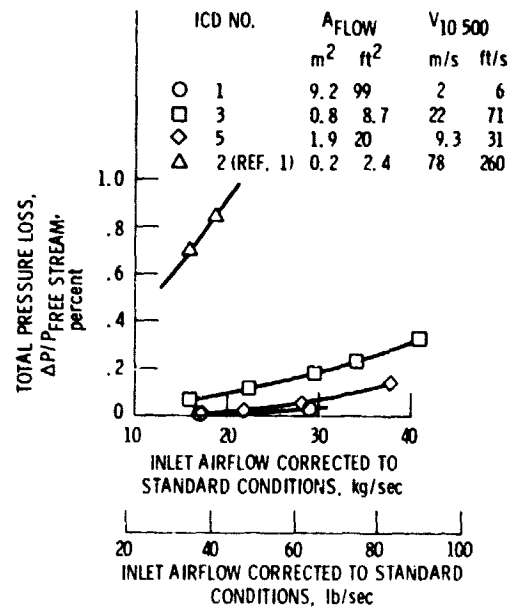
Figure 11. - Pressure loss through ICD's.

INLET

○ WITHOUT ICD
□ WITH ICD

OPEN SYMBOLS SHOW BPF TONE
DARK SYMBOLS SHOW BROADBAND

(a) ICD NO. 1.

(b) ICD NO. 3.

ANGLE FROM ENGINE INLET AXIS, deg

FREE-FIELD SPL FOR 30.5-m (100-ft) RADIUS, STANDARD DAY, dB (RE 2x10⁻⁵ Pa)
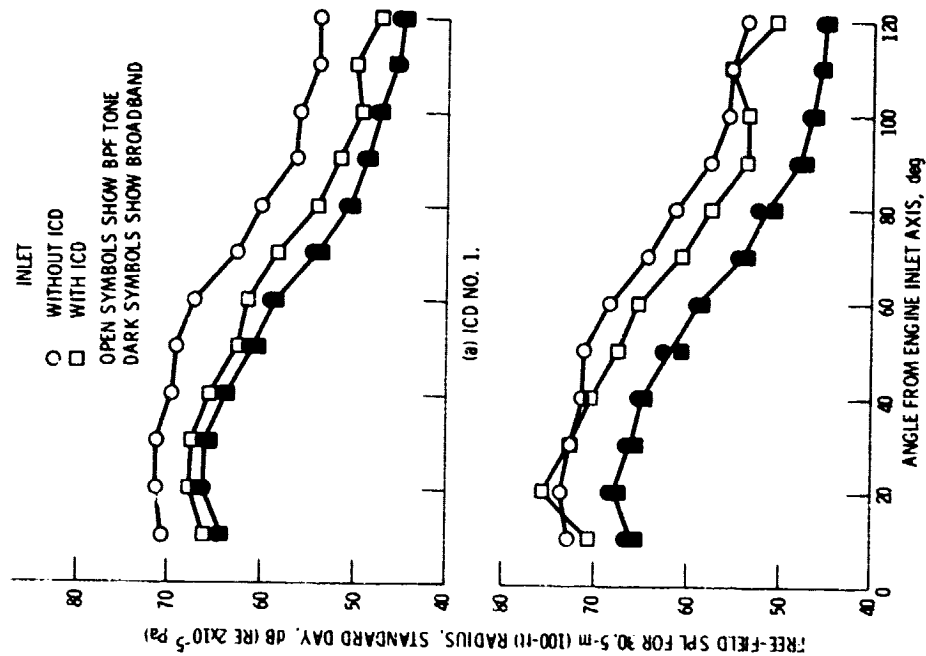
Figure 13. – Far-field directivity patterns at 6750 rpm fan speed.
Analyzer bandwidth 25 Hz.

(a) NO ICD.

NOT
IDENTIFIED BPF_F BPF_C 2xBPF_F BPF_F + BPF_C 3xBPF_F

(b) WITH ICD NO. 1.

FREQUENCY, kHz

SPL, dB (RE 2x10⁻⁵ Pa)
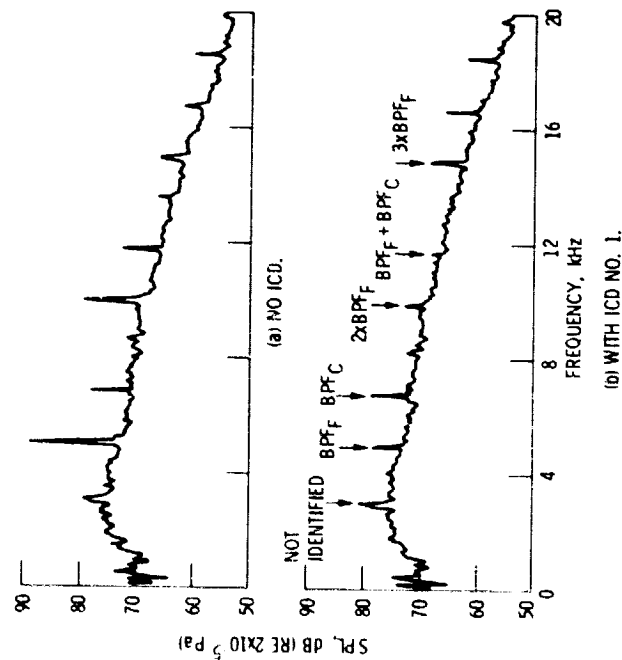
Figure 12. – Narrow-band spectra for ground microphone at 27. 4 m
(90 ft), 40° from engine inlet axis; corrected fan speed 10 500 rpm;
analyzer bandwidth 25 Hz.

FREE-FIELD SPL FOR 30.5-m (100-ft) RADIUS, STANDARD DAY, dB (RE 2x10⁻⁵ Pa)

INLET
○ WITHOUT ICD
□ WITH ICD

OPEN SYMBOLS SHOW BPF TONE
DARK SYMBOLS SHOW BROADBAND

(a) ICD NO. 1.

(b) ICD NO. 3.

ANGLE FROM ENGINE INLET AXIS, deg
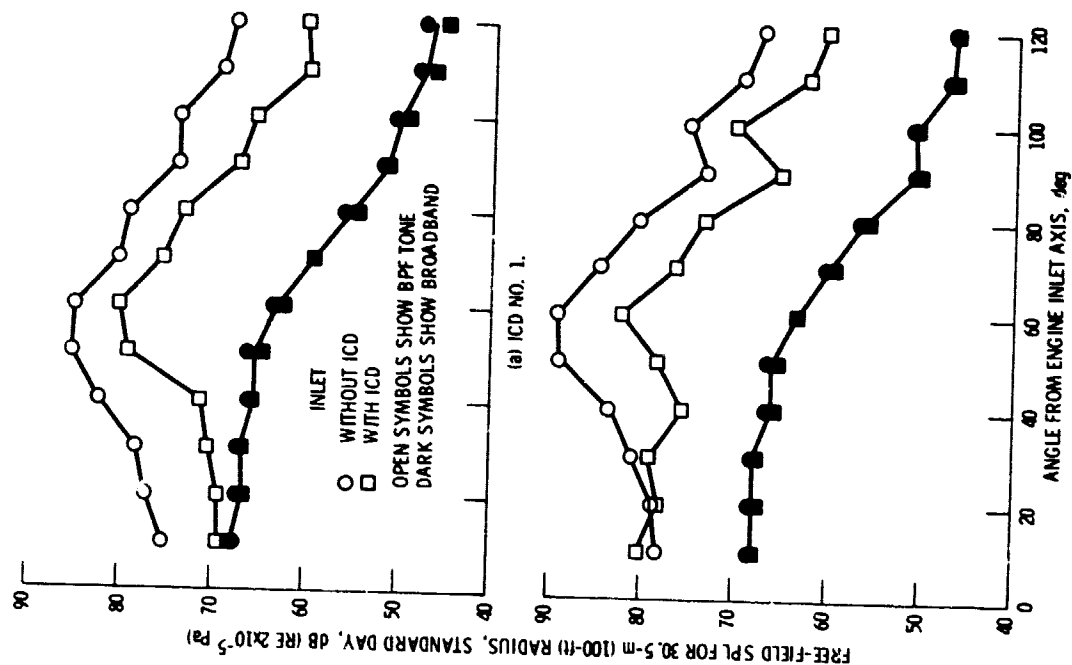
Figure 14. - Far-field directivity patterns at 10 500 rpm fan speed. Analyzer bandwidth 25 Hz.

INLET
○ WITHOUT ICD
□ WITH ICD

OPEN SYMBOLS SHOW BPF TONE
DARK SYMBOLS SHOW BROADBAND

(c) ICD NO. 4.

(d) ICD NO. 5.

ANGLE FROM ENGINE INLET AXIS, deg
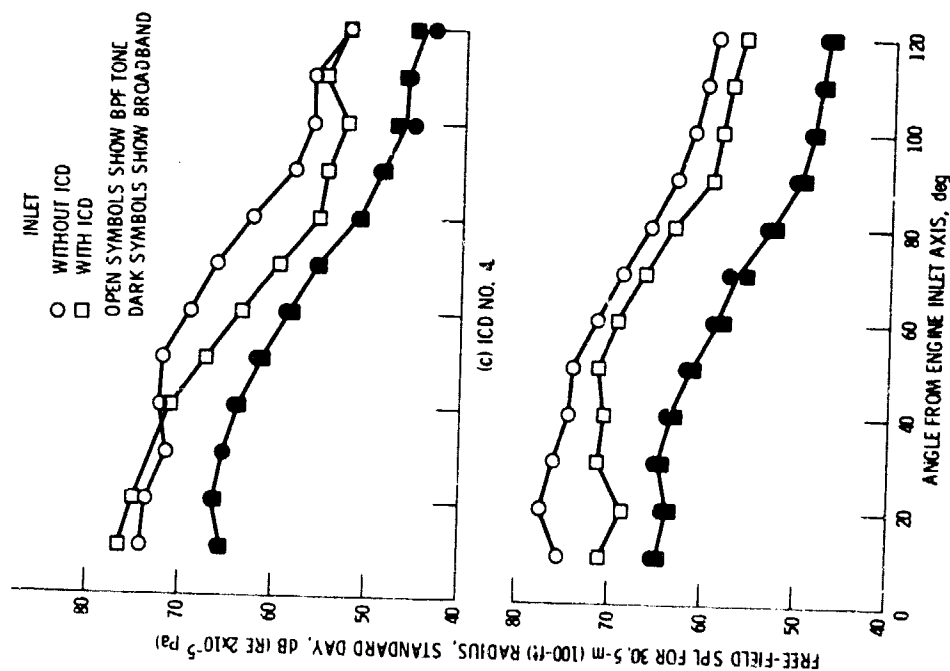
Figure 13. - Concluded.

(c) ICD NO. 4.

(d) ICD NO. 5.
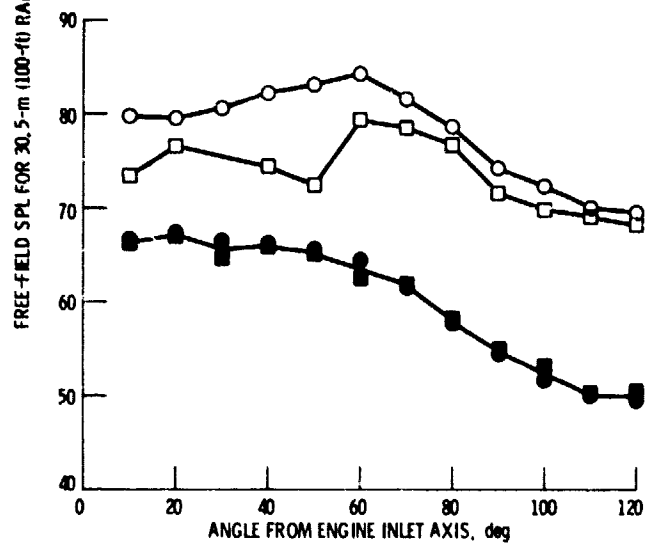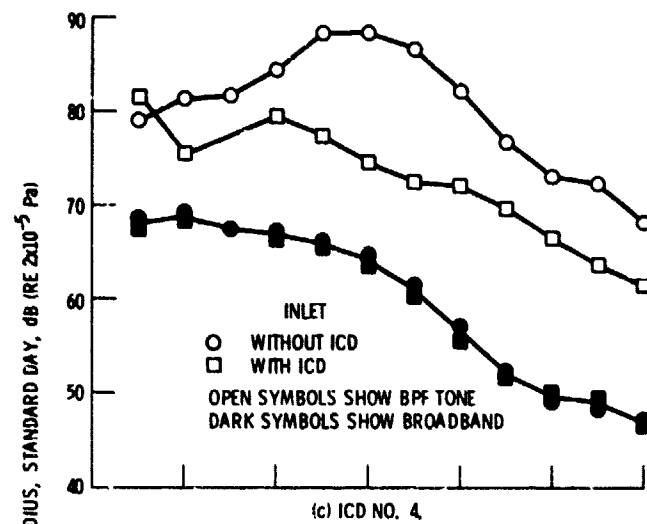
Figure 14. – Concluded.
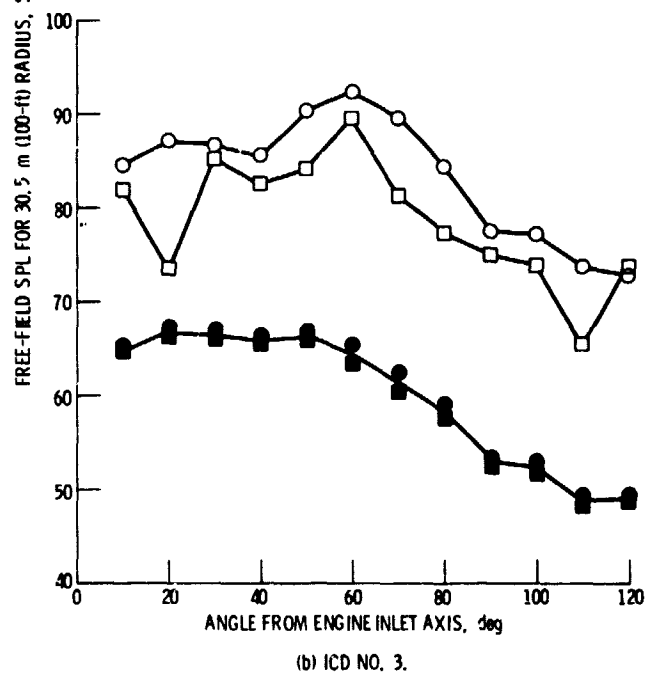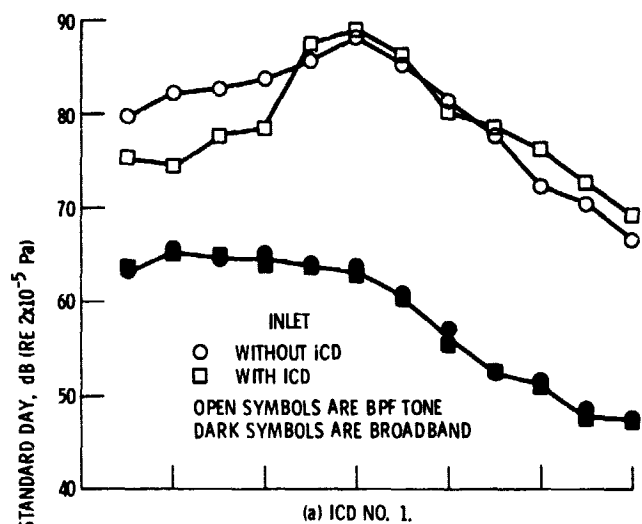
Figure 15. - Far-field directivity patterns at 13 500 rpm fan speed. Analyzer bandwidth 25 Hz.
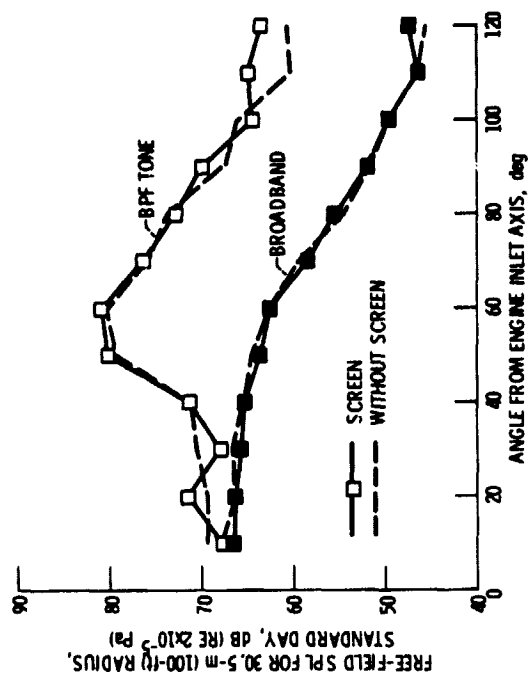
Figure 16. - Effect of additional screen on performance of ICD No. 1. Fan speed 10 500 rpm; analyzer bandwidth 25 Hz.
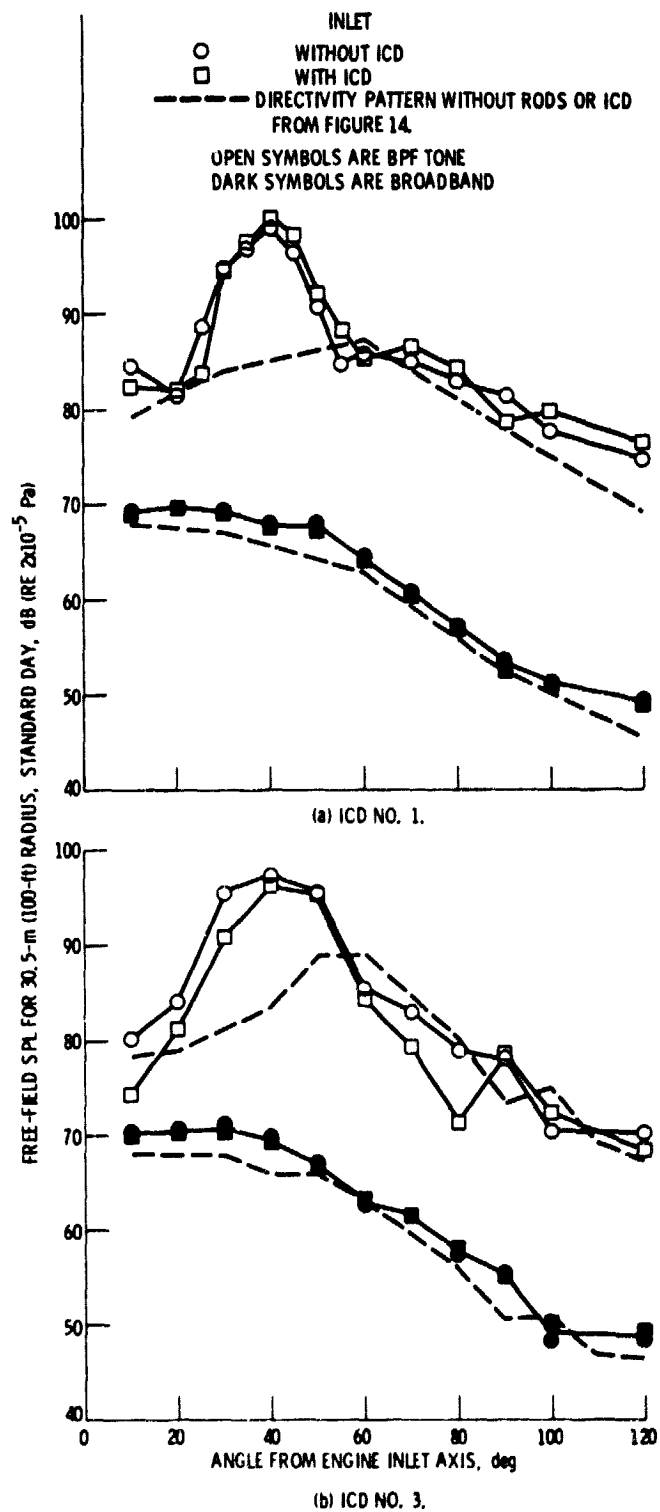

(c) ICD NO. 4.

(d) ICD No. 5.

Figure 15. - Concluded.
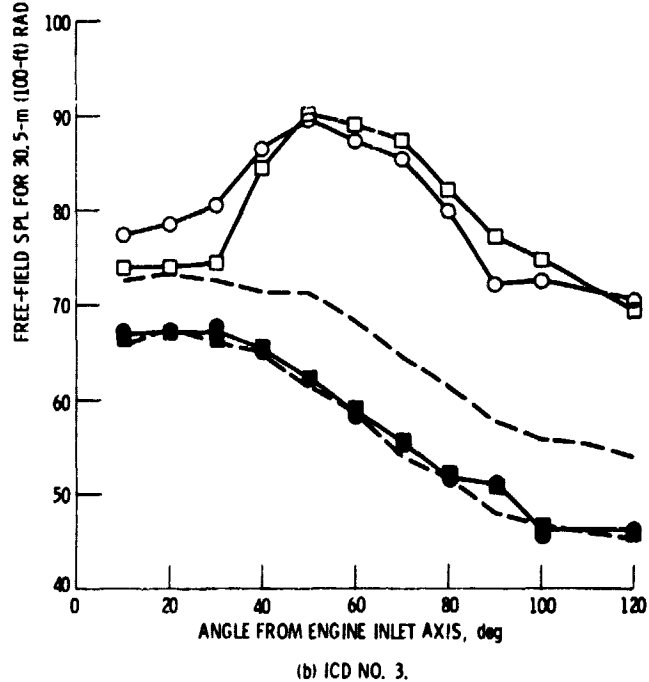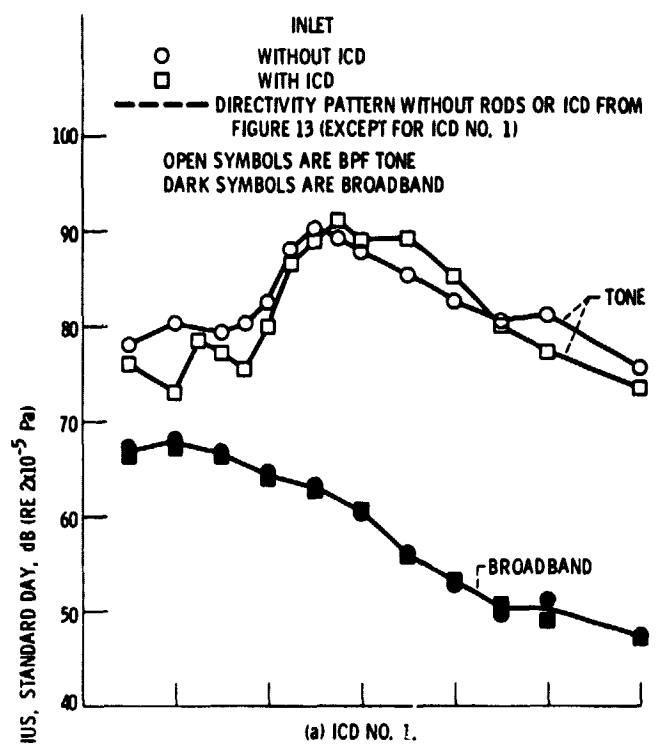
Figure 17. - Directivity patterns for acoustic transmission tests. 41 Rods in inlet; corrected fan speed 6750 rpm; analyzer bandwidth 25 Hz.
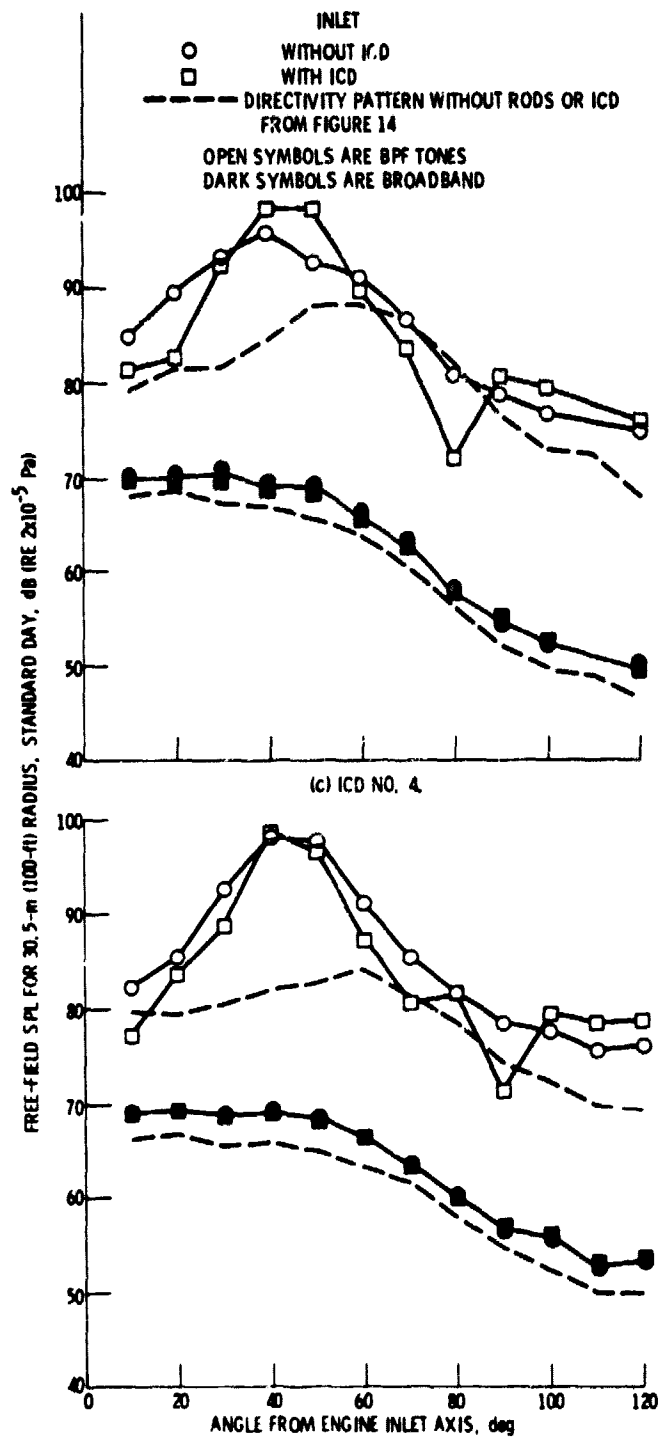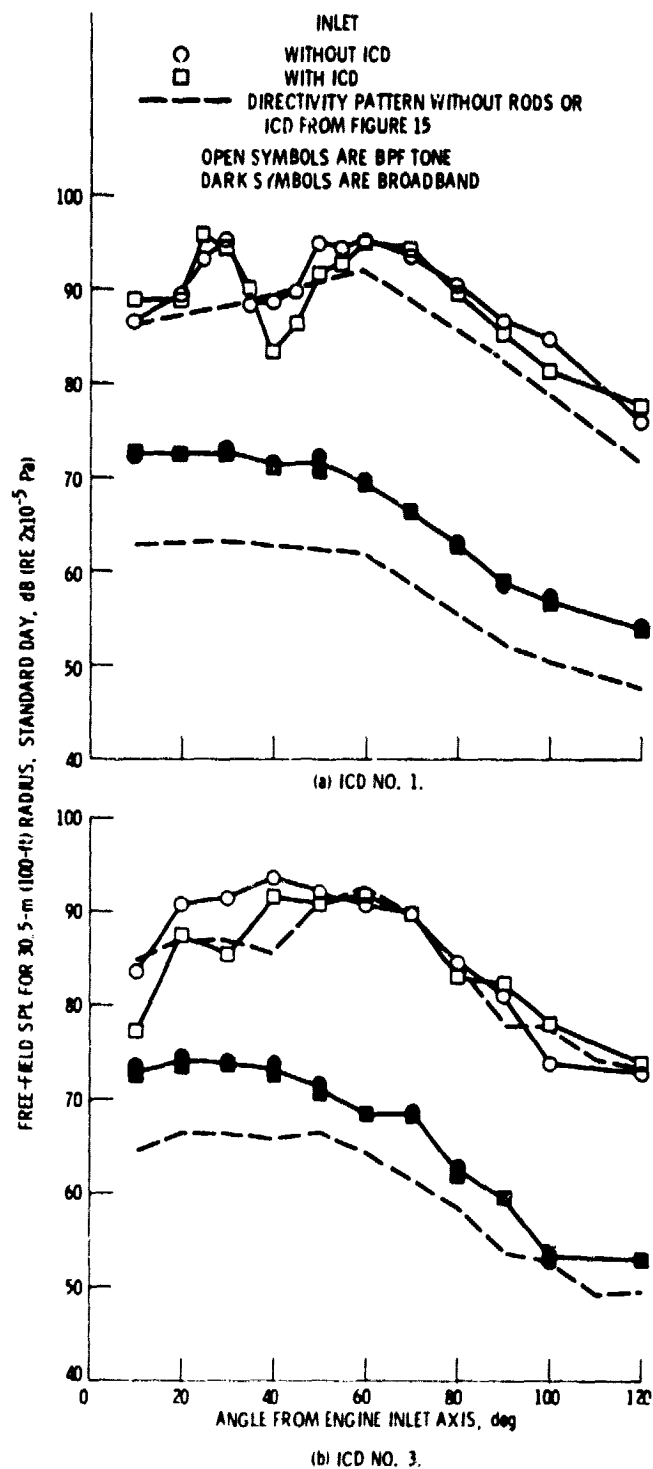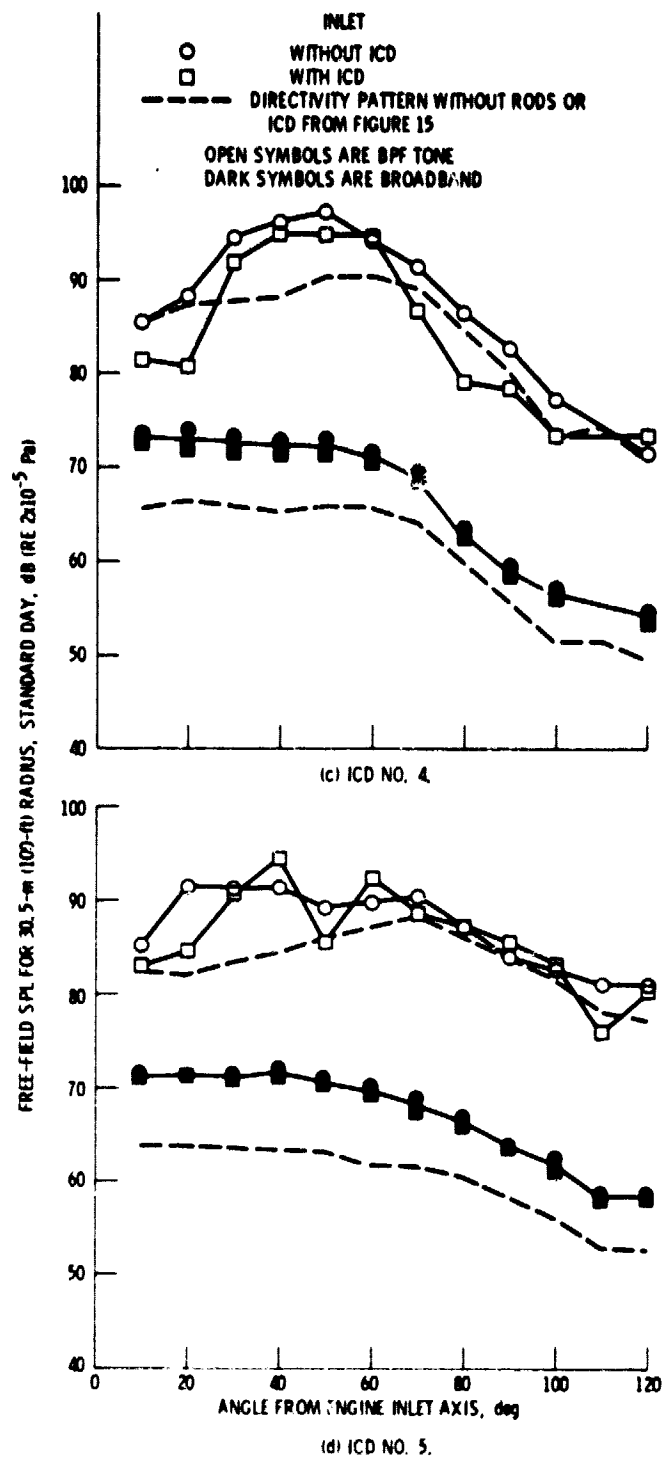
INLET

○   WITHOUT ICD
□   WITH ICD
— — — — DIRECTIVITY PATTERN WITHOUT RODS OR ICD FROM
             FIGURE 13 (EXCEPT FOR ICD NO. 1)

OPEN SYMBOLS ARE BPF TONE
DARK SYMBOLS ARE BROADBAND

(c) ICD NO. 4.

(d) ICD NO. 5.
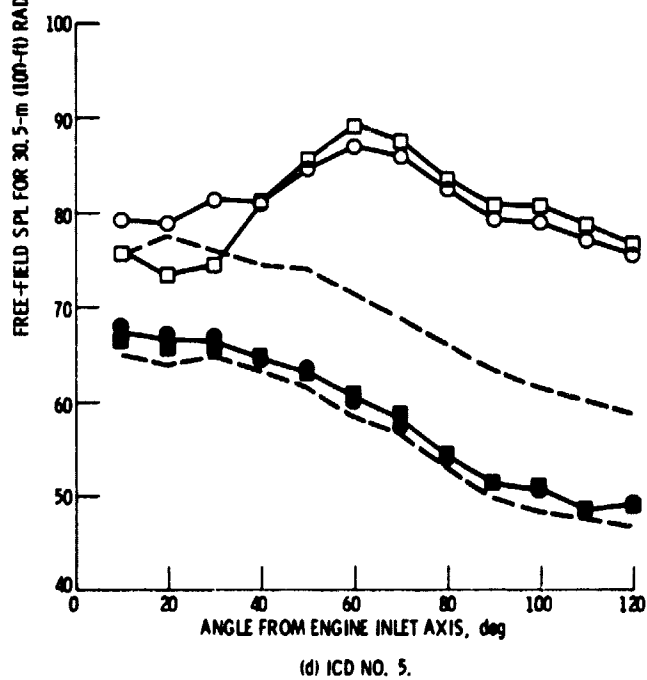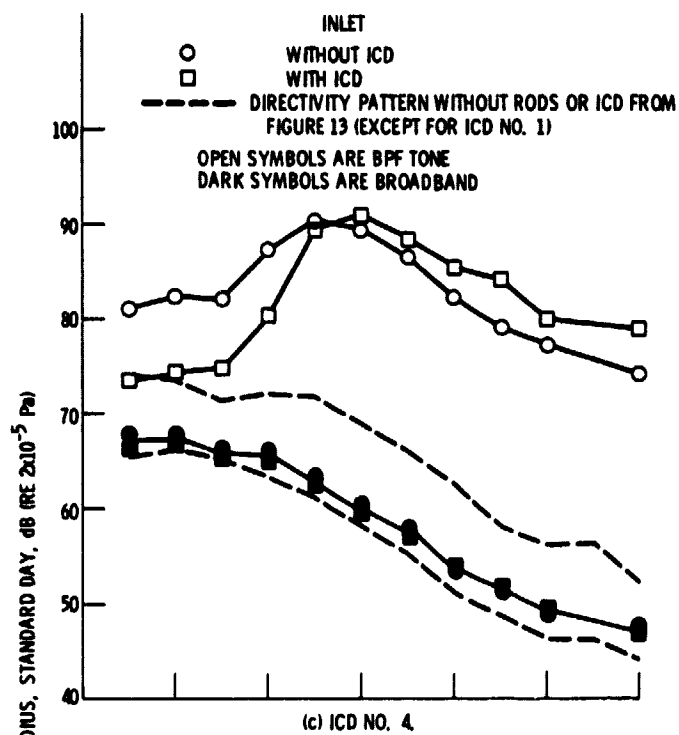
Figure 17. - Concluded.

Figure 18. – Directivity patterns for acoustic transmission tests.
41 Rods in inlet; corrected fan speed 10 500 rpm; analyzer
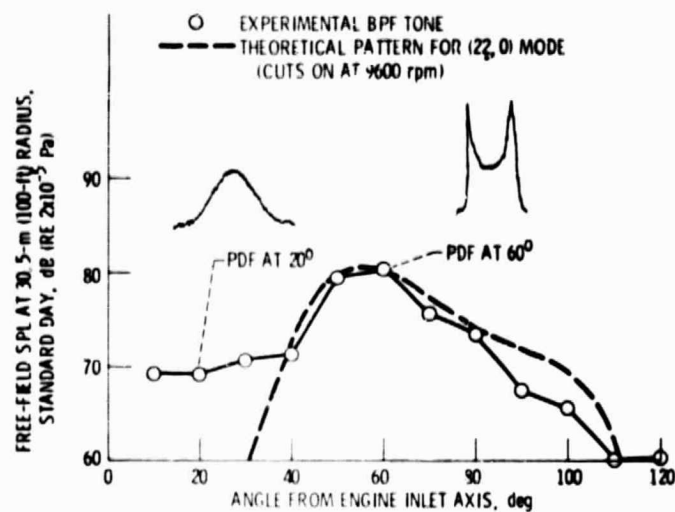bandwidth 25 Hz.

Figure 18. - Concluded.

INLET
○ WITHOUT ICD
□ WITH ICD
— — DIRECTIVITY PATTERN WITHOUT RODS OR ICD FROM FIGURE 15

OPEN SYMBOLS ARE BPF TONE
DARK SYMBOLS ARE BROADBAND

(a) ICD NO. 1.

(b) ICD NO. 3.

FREE-FIELD SPL FOR 30.5-m (100-ft) RADIUS, STANDARD DAY, dB (RE 2x10^{-5} Pa)

ANGLE FROM ENGINE INLET AXIS, deg

Figure 19. - Directivity patterns for acoustic transmission tests. 41 Rods in inlet; corrected fan speed 13 500 rpm; analyzer bandwidth 25 Hz.

INLET
○   WITHOUT ICD
□   WITH ICD
— — — DIRECTIVITY PATTERN WITHOUT RODS OR
        ICD FROM FIGURE 15
OPEN SYMBOLS ARE BPF TONE
DARK SYMBOLS ARE BROADBAND

(c) ICD NO. 4.

(d) ICD NO. 5.

ANGLE FROM ENGINE INLET AXIS, deg

FREE-FIELD SPL FOR 30.5-m (100-ft) RADIUS, STANDARD DAY, dB (RE 2x10^{-5} Pa)

Figure 19. - Concluded.

Figure 20. – Measured and theoretical BPF tone directivity, 10 500 rpm fan speed, ICD no. 1.
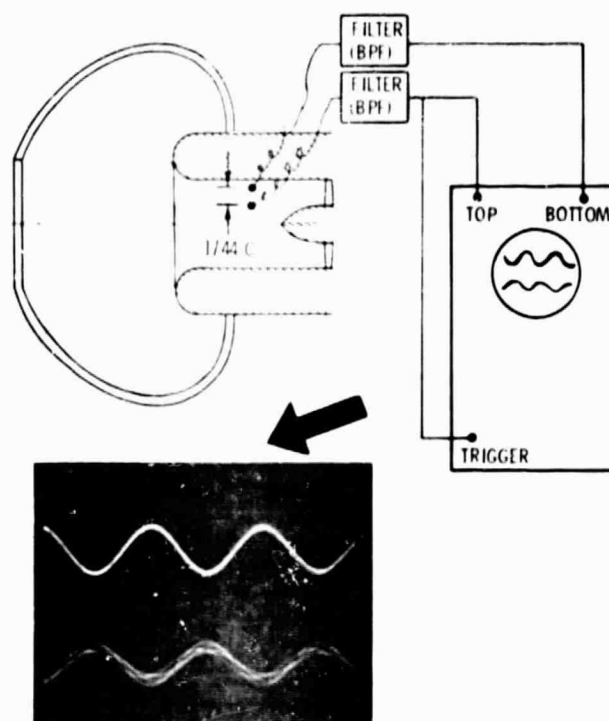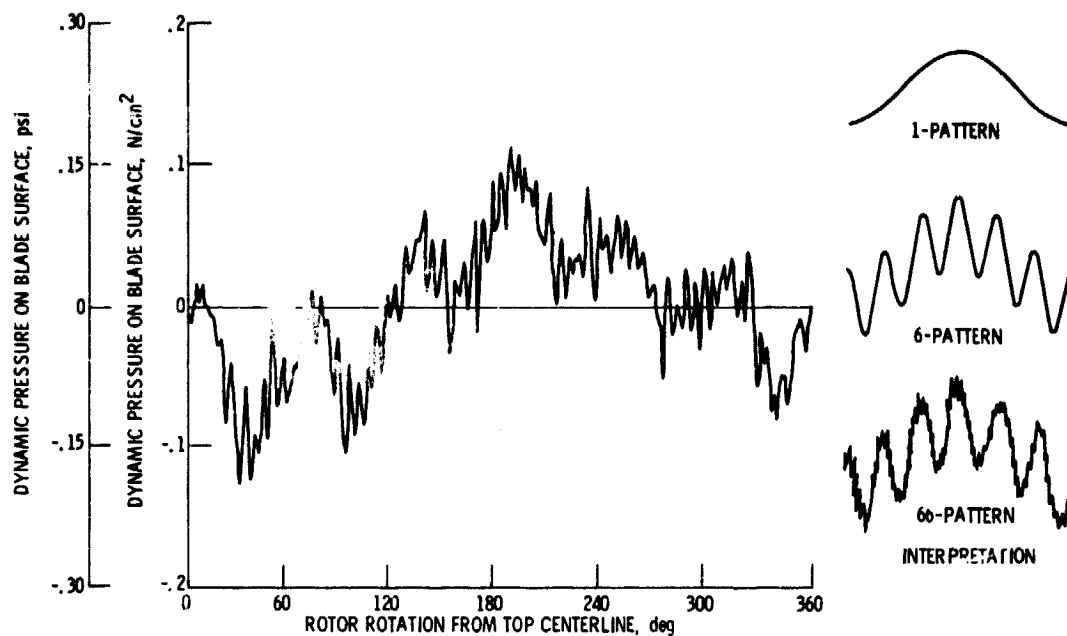

Figure 21. – Experiment to confirm m = 22 mode in duct.

Figure 22. – Pressure waveform averaged over 200 rotor revolutions; transducer B-3; 10 500 rpm fan speed; ICD No. 1.
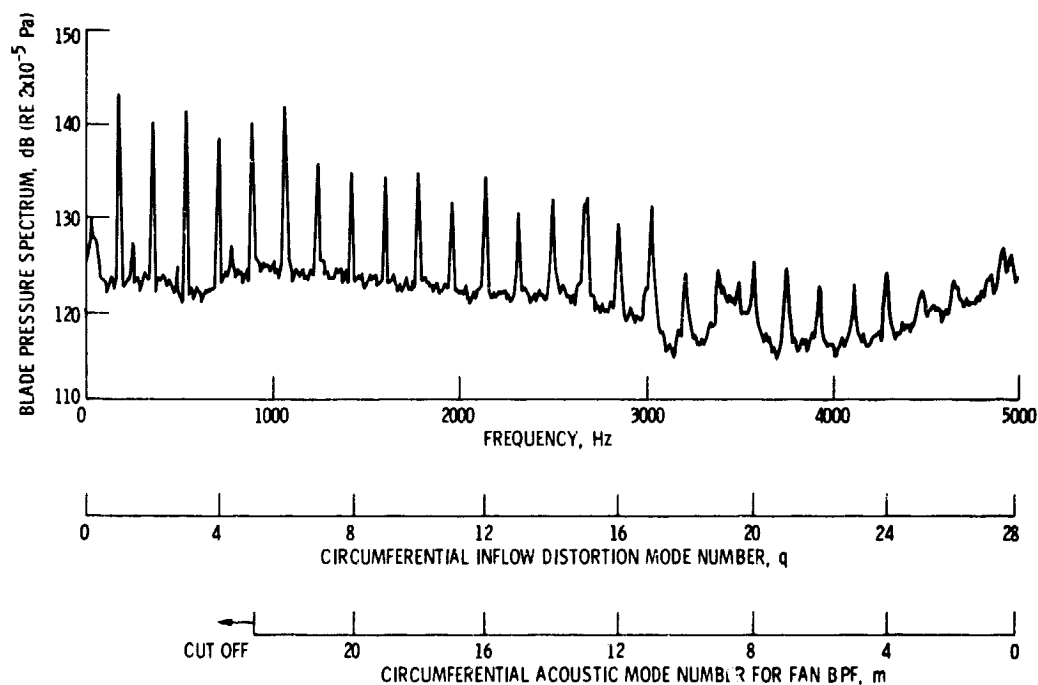
Figure 23. – Blade pressure spectrum for transducer B-3; 10 500 rpm fan speed; n ICD; analyzer bandwidth 6.25 Hz.
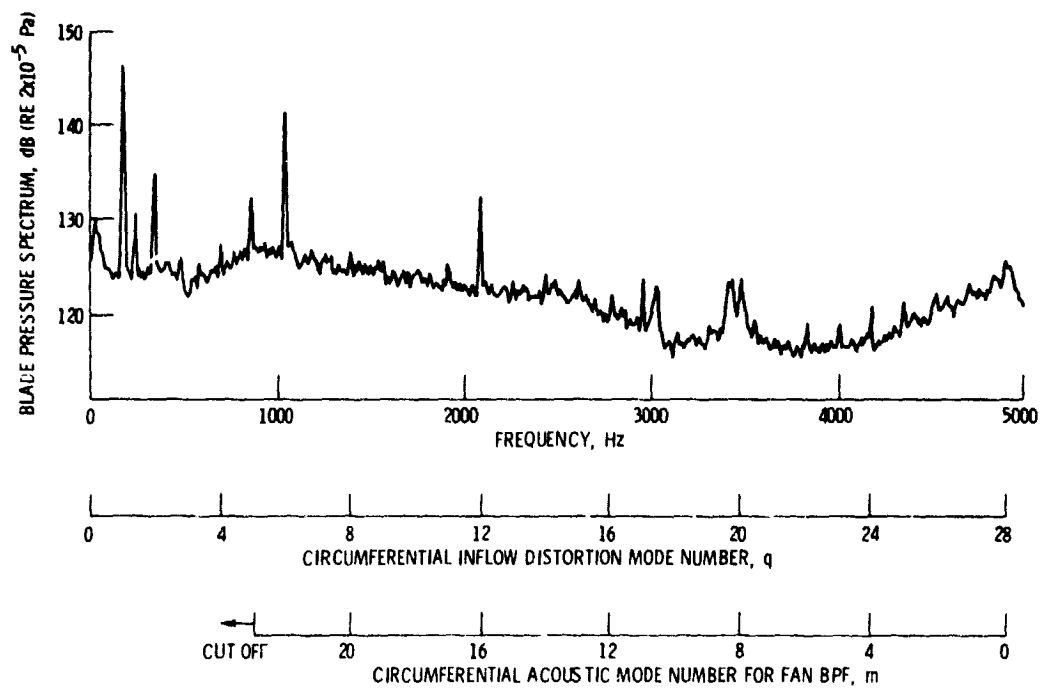
Figure 24. - Blade pressure spectrum for transducer B-3; 10 500 rpm fan speed, ICD no. 1; analyzer band-
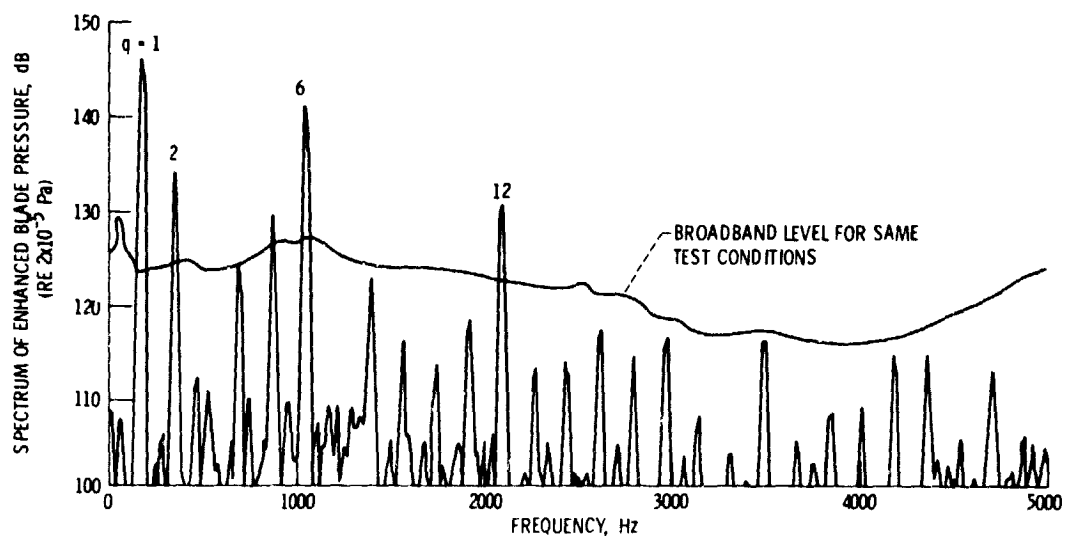width 6.25 Hz.

Figure 25. - Spectrum of enhanced blade pressure signal; transducer B-3; 10 500 rpm fan speed; ICD no. 1;
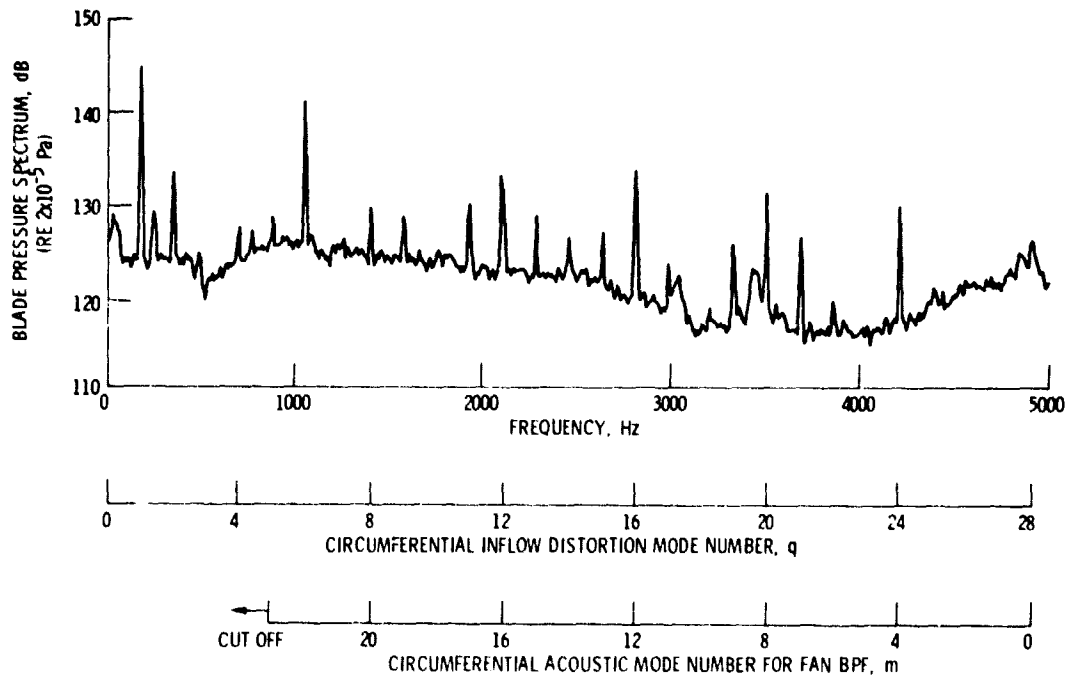analyzer bandwidth 6.25 Hz.

Figure 26. - Blade pressure spectrum for tranducer B-3; 10 500 rpm fan speed; ICD no. 3; analyzer band-width 6. 25 Hz.
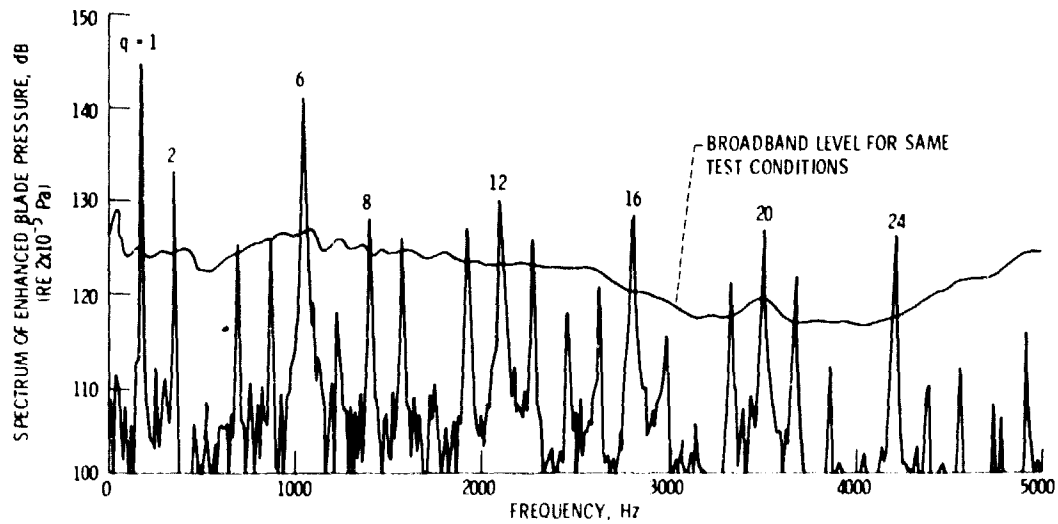

Figure 27. - Spectrum of enhanced blade pressure signal; tranducer B-3; 10 500 rpm fan speed; ICD no. 3; analyzer bandwidth 6. 25 Hz.